Viewing Earth's surface as a soft-matter landscape

Douglas J. Jerolmack[1,2]* *and Karen E. Daniels*[3]*

Abstract | Earth's surface is composed of a staggering diversity of particulate–fluid mixtures: dry to wet, dilute to dense, colloidal to granular and attractive to repulsive particles. This material variety is matched by the range of relevant stresses and strain rates, from laminar to turbulent flows and steady to intermittent forcing, leading to anything from rapid and catastrophic landslides to the slow relaxation of soil and rocks over geologic timescales. From a physics point of view, virtually all Earth and planetary landscapes are composed of soft matter, in the sense that they are both deformable and sensitive to collective effects. Geophysical materials, however, often involve compositions and flow geometries that have not yet been examined in physics. In this Review, we explore how a soft-matter physics perspective has helped to illuminate, and even predict, the rich dynamics of earth materials and their associated landscapes. We also highlight phenomena of geophysical flows that challenge, and will hopefully inspire, work on more fundamental aspects of soft matter.

Upscaling
The application of models derived from small scale dynamics, transferred to larger scales.

Yield stress
The amount of load a material can accommodate without bulk flow arising.

Colloids
Materials composed of one type of microscopic particle dispersed within a second substance, which doesn't easily phase-separate once mixed.

[1]*Department of Earth and Environmental Science, University of Pennsylvania, Philadelphia, PA, USA.*

[2]*Department of Mechanical Engineering and Applied Mechanics, University of Pennsylvania, Philadelphia, PA, USA.*

[3]*Department of Physics, North Carolina State University, Raleigh, NC, USA.*

**e-mail: sediment@sas.upenn.edu; kdaniel@ncsu.edu*

https://doi.org/10.1038/s42254-019-0111-x

Patterns on Earth's surface are created by geophysical flows, which are composed of fluid–particle mixtures of varying proportions, from dry to wet to immersed[1–4] (FIG. 1). These patterns form landscapes that provide the template for human settlement, but their unpredictable dynamics also create natural hazards that threaten lives and infrastructure[5,6]. Familiar features such as canyons, sand ripples, dunes, river channels and deltas also form in the deep ocean[7,8] and are common in the solar system[9]. The apparent universality of these features, despite the exotic nature of some fluid and solid materials involved, such as liquid methane and water-ice particles on Titan, is a motivation to understand the underlying physics[10].

The study of the geological landscapes — the 'science of scenery'[11], known as geomorphology — faces a central challenge of understanding and linking the mechanics of geophysical flows to the evolution of landscapes that results from the cumulative effects of numerous flow events[12]. The challenge arises because the microscopic physics of complex fluid–particle flows are not fully understood, and the usual difficulties in upscaling are compounded in complicated geological systems. Accordingly, researchers often seek parameterized expressions that relate sediment-transport rates to suitably averaged applied stresses, and which are calibrated to field-scale observations[13]. Although rooted in some physical processes, sediment-transport equations are inherently phenomenological: they are often designed for simplicity so that they can be inserted into spatially distributed numerical models to simulate landscapes. An important requirement of these models is to assign a criterion for the onset of failure and erosion of earth materials, a notoriously difficult problem[14].

These problems and approaches in geomorphology have parallels in soft-matter physics, for which two key goals are developing bulk rheological relations for complex fluid–particle systems and understanding the emergence of a yield stress. Furthermore, earth materials exhibit such soft-matter effects as shear-rate-dependent rheologies influenced by microstructure[15–18]; ageing and history dependence in colloids and granular materials[19–25]; and signatures of glassy dynamics and jamming[26–30]. As such, some of the same underlying causes that have engaged soft, condensed-matter physicists — excluded-volume effects, the emergence of bulk properties such as rigidity from particle-scale interactions and the role of disorder in dynamical phase transitions — are also at play in sculpting the landscapes of Earth and elsewhere. Another key feature that is common across studies of soft-matter systems[31,32] is a focus on the properties and behaviour of disordered materials, which earth materials surely are. Our Review emphasizes that some of the central questions in soft-matter physics today are also central questions in geophysical flows: how the microstructure and resultant rheology of earth materials are influenced by polydispersity in particle size and shape, and inter-particle attraction; the sensitivity of ageing and history dependence to inter-particle interactions, initial conditions and flow geometry; and the role of mechanical perturbations on creep, flow and the transition between these states.

Key points

- Earth and planetary landscapes are created by the erosion and deposition of particulate material; this discipline is called geomorphology.
- Soil, rocks and ice relax over geologic timescales, but may also fluidize under shear or lubrication; thus, glassy dynamics, rigidity transitions and rheology are central concepts.
- Progress in soft-matter physics can be extended to improve the understanding of geophysical flows that shape landscapes.
- Landscapes present a wider range of material heterogeneity, system geometry and excitations than have been examined in physics experiments, presenting new challenges and opportunities.
- Soft-matter physics and geomorphology are long-lost relatives, and we outline promising avenues for reunification and collaboration.

However, geophysical flows of granular materials are far from the idealized granular flows and suspensions usually considered in physics (FIG. 1). Particulate earth materials typically have strong heterogeneity in grain size and composition, are often cohesive and their dynamics occur on a vast range of pressures and timescales. Although granular effects in these flows are often dominant, more complicated inter-particle interactions — such as chemical, electrostatic and thermal effects — may also be important (FIG. 1). Moreover, these materials are subject to time-varying and space-varying forcing, such as rainfall, wind and water currents, and motion of tectonic plates. Particles may also break or deform under sufficiently high collision energy[33,34]. Perhaps most challenging and intriguing is that geophysical flows make their own boundaries[33]: flows both respond to and also create landscape patterns. In spite of these differences, recent experimental advances in the field are illustrating how emerging unifying concepts in soft matter can be meaningfully applied to describe natural landscapes and also how landscapes can present as-yet-unstudied materials and experimental configurations that may challenge and illuminate the fundamental physics.

The application of granular physics to understanding fault dynamics and earthquakes is well established[35–39]. The importance of granular contributions to geomorphology is only starting to gain attention[14,28,33]. Consideration of other relevant soft-matter effects, such as glassy dynamics and colloidal gel formation, is rarer still. Indeed, the dominant framework for describing particulate (sediment) transport has been fluid mechanics, and for good reason: water and wind form turbulent boundary-layer flows on Earth's surface, which produce time-varying and space-varying stresses that entrain and suspend particles[3,40,41]. Even in the absence of a real fluid, high-concentration particulate flows such as landslides can be described as viscoplastic fluids[14,42,43].

The scope of our Review is framed by this context, as well as studies presenting successful complementary views on geomorphology, most notably: the formal statistical mechanics formulation of sediment transport by David Furbish and colleagues[44,45], and related probabilistic and stochastic approaches in geomorphology[46–49]; nonlinear and dynamical-systems approaches to landscape pattern formation[50–53]; hydrodynamic and classical stability analyses[3,4]; and reviews justifying the applicability of small-scale experiments to natural landscapes[54,55]. However, we focus our attention on particulate systems, in which lessons from granular materials and suspensions translate most directly to geophysical systems. Nonetheless, clear connections also exist to other amorphous earth materials, such as rock and ice. Although we emphasize granular effects, additional particle interactions are also considered, especially in cases where they give rise to poorly understood cohesive or rheological behaviours in particulate geophysical flows. For many of these topics, there are existing reviews of key soft-matter concepts and techniques that we recommend: on rheology and yielding in soft materials[56–61] and their application to geophysical flows[14,33]; jamming[62] and glassy dynamics[29,57,61]; granular segregation[63]; and a variety of experimental soft-matter[32] and granular[64] techniques.

In this Review, we first classify geophysical flows in terms of dimensionless strain rate and solid volume fraction. We then outline soft-matter physics concepts that find application in the study of earth materials, before discussing case studies and outstanding problems in this field of research.

Classification of geophysical flows

Earth is 'soft' on geological timescales if we take the meaning of that term in the spirit of Pierre-Gilles de Gennes[65]: the ground is composed of materials that are responsive in their collective effects. However, only the patient observer will notice the relaxation of mountains as rocks flow at speeds of 10^{-1} nm s^{-1} (10^{-2} m y^{-1}). Slightly faster are the rates at which soil and ice creep downhill, sometimes exceeding 10^{2} nm s^{-1} (10^{1} m y^{-1}). Yet, true to the typical sensitivity of soft materials, these processes can intermittently become unstable and landslides can reach speeds of 10 m s^{-1} (FIG. 1). It is helpful to categorize these flows in terms of phenomenology and dynamics.

Phase space. The particulate geophysical flows that are discussed in this Review can be positioned in the phase space of two parameters: the dimensionless strain rate $I \equiv \dot{\gamma} t_{micro}$, where $\dot{\gamma}$ is strain rate and t_{micro} is a microscopic timescale of particle motion[60,66,67]; and volume fraction ϕ (BOX 1; FIG. 1). Note that at least one additional dimensionless number is implicit in this classification: the collision Stokes number, $\mathrm{St} = (\rho_p - \rho_f) d u / \eta_f$, where ρ_p is particle density, ρ_f is fluid density, d is particle diameter, u is particle velocity and η_f is fluid viscosity[33,68]. In the limit $\mathrm{St} \gg 1$, in which collisions dominate, $I = I_i$ is the inertial number, whereas in the low-St limit, in which fluid viscosity damps particle collisions, $I = I_v$ is the viscous number[33] (BOX 1). In addition, there are other dimensionless numbers that are required to fully characterize specific classes of flows[33,42,69]. A final comment about the limitations of this parsimonious classification is that both I and ϕ are diagnostic rather than prognostic. These variables are helpful for describing flows, but it is not possible to predict a priori what the shear rate and volume fraction of a self-formed geophysical flow will be. Nonetheless, presenting these geophysical systems in I–ϕ space is useful for showing how particle concentration relates to shear deformation and flow. For self-formed geophysical flows, these two variables co-evolve in space and time.

Glassy dynamics
Extremely slow dynamics (creep) observed in disordered materials in the vicinity of yielding.

Jamming
The development of a finite yield stress in an idealized, disordered material; the transition from a flowing to a rigid state.

Rigidity
Ability to support a finite stress without inducing bulk flow.

Disordered materials
Solid materials in a non-crystalline state.

Rheology
The science relating how external forces cause material deformation, including the rate-dependence of these effects.

Creep
Small deformation or motion of the particles within a solid, occurring below yield.

Thermal effects
Effects arising when the thermal fluctuations on the constituent particles in the material are of non-negligible magnitude; this corresponds to low Pēclet number.

Colloidal gel
Colloidal system consisting of attractive or cohesive particles dispersed in a liquid, at a volume fraction that is above the rigidity transition.

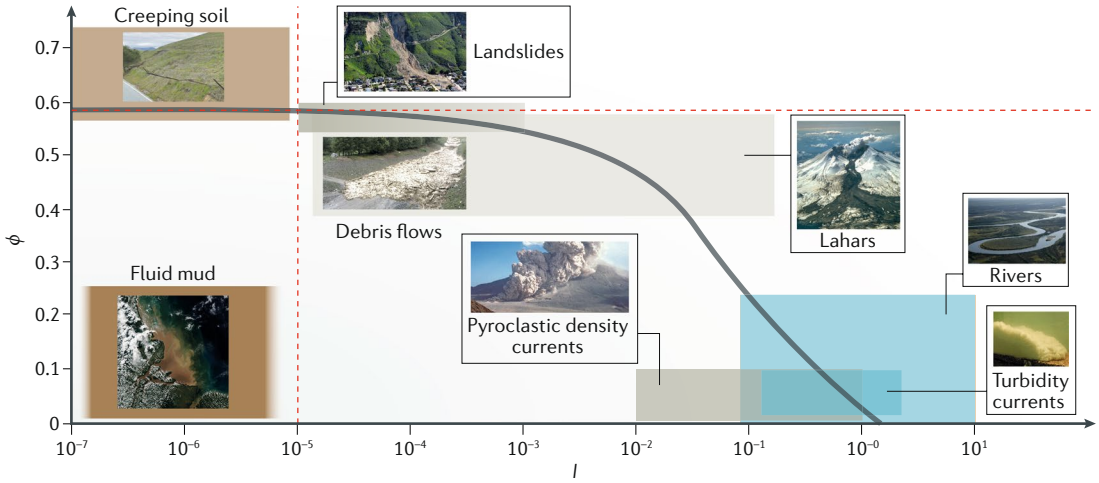

Fig. 1 | **Phase diagram of particulate geophysical flows, parameterized by dimensionless shear rate *I* and solid volume fraction ϕ.** The boxes mark the typical ranges of parameters in which each type of bulk flow is observed, based on values reported in the literature and assuming that confining pressure is hydrostatic. Representative images associated with each flow are also shown. Brown boxes correspond to soil or mud systems that are solid (or solid-like), grey boxes are particulate flows with little or no water that are typically gravity-driven and blue boxes are suspensions (granular gases) for which hydrodynamic stresses from water are dominant. Boundary values for *I* for fluid muds are completely unknown, as is the lower bound for creeping soil. The two red dashed lines mark the approximate boundaries of the solid–fluid transition: the yielding line for $I \sim 10^{-5}$ is determined from REFS[16,30], and the critical volume fraction 0.59 is chosen from experiments of REF.[67]. The solid grey line indicates a proposed $\mu(I)$-type relation (BOX 1) to guide the eye (μ is an effective friction coefficient); it follows data from experiments on fluid-sheared sedimenting particles[16]. Note that fluid muds, in which cohesive or attractive particle interactions are significant, do not fall on the grey line, indicating major deviations from $\mu(I)$ rheology. Creeping soil image capture: April 2019 © 2019 Google. Landslides image is reproduced courtesy of Mark Reid, USGS. Debris flow image is reproduced courtesy of the Agency for Civil Protection – Autonomous Province of Bolzano. Lahars image is reproduced courtesy of Tom Casadevall, USGS. Pyroclastic density currents image is reproduced courtesy of Peter Lipman, USGS. Rivers image is reproduced courtesy of Steve Hillebrand, USFWS. Turbidity currents image is republished with permission from ASCE, from Characteristics of velocity and excess density profiles of saline underflows and turbidity currents flowing over a mobile bed, Sequeiros et al., 136, 412-433 (2010; REF.[272]); permission conveyed through Copyright Clearance Center, Inc. Fluid mud image is reproduced courtesy of NOAA.

Geophysical flows. The flows that we consider in this Review are:

- Soil creep is the sub-yield, quasi-static, downslope motion that occurs on hillsides[70–73]. Creep corresponds to the largest ϕ values and smallest *I* values; the lower bound of *I* is unknown due to measurement limitations, but it is many orders of magnitude smaller than the range shown in FIG. 1 (REF.[30]).
- Landslides are dry to partially wet, dense granular flows that move down hillsides; the lower ϕ than that of creeping soil arises because shear results in dilation of the flow[42,74,75].
- Debris flows are dense granular suspensions, often formed from progressive wetting of landslides, which typically move down river channels[42,43,76].
- Lahars are essentially debris flows formed by rapid wetting of volcanic deposits, but are sometimes reported to have larger runout distances, owing to the presence of fine ash[33]. For this reason, we have placed them in the same regime of the I–ϕ phase diagram as debris flows, with a similar range of ϕ and filling out the large-*I* range (FIG. 1).
- River flows have average particulate concentrations that are typically in the very dilute suspension regime, but may reach moderate density suspensions in some cases. However, rivers drive interfacial flows of dense-granular and creep regimes at their boundaries, as discussed below (FIG. 2).
- Turbidity currents are particulate suspensions with buoyancy contrast sufficient to drive flow, but for which ϕ is low enough that turbulence is sufficient to keep the grains suspended[77,78]. They typically form in the ocean from the collapse of granular material and subsequent (turbulent) entrainment of ambient water[40,77–79].
- Pyroclastic density currents arise when explosive volcanic eruptions create mixtures of hot gas and particles that are denser than ambient air. The estimated range of bulk values for ϕ and *I* (REFS[33,69]) is not dissimilar to that of turbidity currents. Like rivers, these dilute density currents have high-concentration (dense-granular) flows at their base. Ash particles in these flows are sensitive to electrostatic effects that may induce substantial aggregation[69].
- Fluid muds are another example for which electrostatic effects are relevant. They are dilute to moderately dense, quasi-stable, colloidal gels[59,80] that form in estuaries and coasts from cohesive clays and organic materials delivered by rivers[81,82]. Interparticle attraction among the associated fine grains is induced when particles enter salty water and the typically repulsive surface charges are screened by

dissolved ions[81,83]. Although the bounding values of I are unknown for such flows, attractive particle interactions allow a yield stress to develop at lower-than-expected ϕ values[82].

Classification based on dynamics. Deformation of soft materials is exquisitely sensitive to the nature of the forcing and to boundary conditions. Geophysical flows may be usefully placed into two broad categories based on their dynamics (FIG. 2). In an interface-driven flow, energy transfer at the interface between two materials with contrasting densities causes the shape of the interface to evolve in both space and time. These driven dynamics can give rise to characteristic interface shapes, including well-defined wavelengths, as is common in non-equilibrium systems[84]. In some cases, a moving fluid can push the interface into a new shape, as occurs for ripples on the surface of cooling lava[85,86]. The more common situation on Earth's surface is fluid-driven sediment transport, such as wind-blown sand on the surface of dunes[1,87], underwater sand ripples and dunes[4,88], turbidity currents[77,78] and meandering river channels[3,89], all of which involve both erosion and redeposition of particulate material along the interface.

Modelling efforts for such systems have traditionally focused on describing the evolution of the shape of the interface, rather than the evolution of the bulk material underneath[3]. Mechanics-based formulations for sediment transport envision a thin film of particles, with momentum supplied from the driving fluid, transported over a static underlying bed[22,90,91]. The separation between this flowing bed-load layer and the substrate,

Box 1 | **Rheology of soft materials and earth materials**

Rheology relates applied forces to the resulting deformation of a material, for instance, via shear stress τ and strain rate $\dot{\gamma}$. One simple example, relevant for fluids, is the Herschel–Bulkley relation,

$$\tau = \tau_y + C\dot{\gamma}^n \quad (1)$$

where τ_y is the yield stress. For a Newtonian fluid, $\tau_y = 0$ and $n = 1$, in which case, $C = \eta_f$ is the viscosity. For shear-thickening fluids, $n > 1$ and the apparent viscosity increases with shear rate; for shear-thinning fluids, $n < 1$ and the apparent viscosity decreases with shear rate. Owing to its flexibility, Eq. 1 has been used to describe a wide range of soft materials. However, the physical origins of τ_y and n vary widely among systems and, for the most part, remain to be understood[56,59,250]. The addition of particles to a Newtonian fluid creates a suspension that, at high particulate volume fraction ϕ, can be modelled as a single-phase, non-Newtonian fluid. Natural and experimental debris flows typically behave as shear-thinning, yield-stress fluids with behaviour described by Eq. 1 (REF.[83]).

The Herschel–Bulkley equation may be non-dimensionalized by a confining pressure (normal stress) P_p, which re-casts the relation in terms of friction $\mu \equiv \tau/P_p$ and a non-dimensional shear rate, which is the viscous number, $I_v = \eta_f \dot{\gamma}/P_p$ (REFS[60,67])

$$\mu = \mu_s + I_v^n \quad (2)$$

where $\mu_s \equiv \tau_y/P_p$ is a static friction coefficient; from the perspective of yield-stress fluids, the effective static friction arises from a cooperative effect of many particles. For viscous granular (that is, non-inertial and athermal) suspensions, it has been proposed that the effective friction results from effects on two timescales. $t_{micro} = \eta_f/P_p$ is a viscous drag timescale for a suspended particle and $t_{macro} = 1/\dot{\gamma}$ is the strain timescale for rearrangement of grains around a particle[67]. Accordingly, the constitutive relations for shear stress and volume fraction become functions of $I_v = t_{micro}/t_{macro}$

$$\tau = \mu(I_v)P_p \text{ and } \phi = \phi(I_v) \quad (3)$$

Functional forms have been derived for Eqs. 2 and 3, which fit the behaviour of a wide range of viscous granular suspensions[60,67]. This rheology has been extended to accurately describe the dense to dilute regimes of fluid-driven sediment transport[16,93]. For flows in which collisions dominate over fluid viscosity, the strain timescale remains the same but the relevant microscopic timescale for grain motion is inertial, that is, $t_{micro} = \sqrt{d^2\rho_p/P_p}$, where d is particle diameter and ρ_p is particle mass density[33]. Different functional forms for Eqs. 2 and 3, with an inertial number I_i in place of I_v, describe a wide range of inertial granular flows[66] and also natural landslides[30]. Importantly, functional relations based on Eq. 3 all exhibit effective friction that converges to the static value in the limit of vanishing shear rate. This yield transition is associated with a packing fraction that approaches the critical value ϕ_c associated with jamming[62,67]. These relations are collectively referred to as $\mu(I)$ rheology.

In repulsive colloidal suspensions, the excluded-volume effects that dominate $\mu(I)$ rheology at high ϕ values remain relevant. However, thermal effects introduce an additional relaxation timescale, such that high-ϕ colloidal glasses are typically considered to be distinct from granular systems in terms of yielding[56,59]. Nonetheless, simulations show that $\mu(I)$ may be generalized to repulsive colloidal glasses by explicitly accounting for thermal effects via a Péclet number[242].

Other classes of soft matter may be created by combinations of the above-mentioned classes. One example relevant for geophysical flows is granular suspensions in yield-stress fluids, recently examined by adding repulsive and athermal particles to non-Newtonian emulsions[241]. Excluded-volume effects influence the yield stress and effective viscosity, independently of the suspending fluid composition. Accordingly, Eq. 1 generalizes as

$$\tau = \tau_{y,\phi}(\phi)\tau_y + C_\phi(\phi)C\dot{\gamma}^n \quad (4)$$

where τ_y, C and n are properties of the suspending fluid, and $\tau_{y,\phi}(\phi)$ and $C_\phi(\phi)$ are dimensionless functions that increase monotonically from 1 with increasing ϕ. As with Eq. 1, Eq. 4 may be re-cast in terms of $\mu(I)$ rheology[241]. This model has relevance for natural debris flows, which often consist of dense mud suspensions that carry boulders.

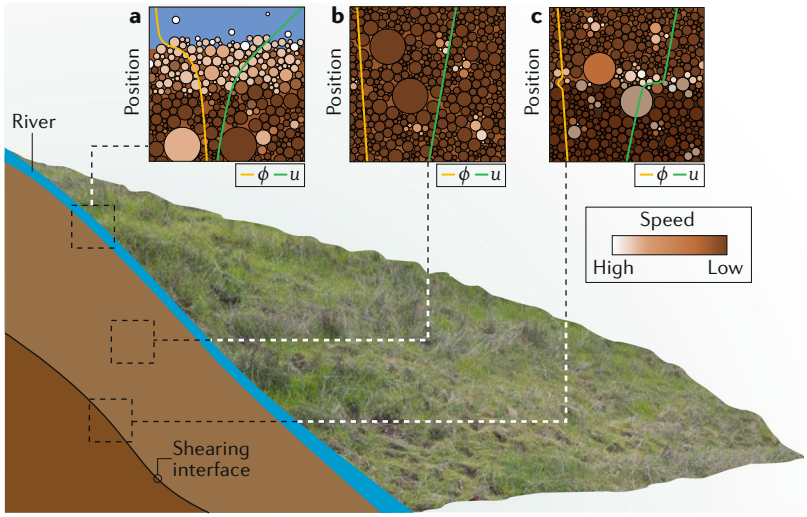

Fig. 2 | **Interfacial and bulk dynamics of geophysical flows illustrated on a prototypical soil-covered hillslope.** Each inset has schematic log-linear profiles of particulate volume fraction ϕ and downslope velocity u overlaid; grain colour is relative speed. **a** | The blue region represents a small river, an example of an interface-driven flow in which fluid shear from above drives deformation of the particle–fluid interface; granular shear drives motion deep into the substrate, which transitions at depth to creep[16,92]. **b** | Gravity-driven bulk deformation of the polydisperse granular soil; the example shows soil creep, which is accommodated by local and rare rearrangements as the landscape relaxes in response to disturbance. Both u and ϕ are typically observed to decrease exponentially with depth, owing to granular friction (for u) and compaction (for ϕ). **c** | A shearing interface accommodated by dilation appears where local rearrangements critically percolate to facilitate slip; this is often the base of catastrophic failure. Figure courtesy of Andrew Gunn, University of Pennsylvania, USA. Hillslope image capture: April 2019 © 2019 Google.

however, is not so sharp in reality; motion of grains at the interface induces motion of grains in the bulk via granular shear, inducing creep deep beneath the bed[92–94] (FIG. 2a). Thus, the fluid–particle interface is fuzzy and it grows or contracts with changes in the applied fluid stress[92,95,96]; nevertheless, the particulate transport is boundary-driven.

This scenario is in contrast with earth materials undergoing bulk flow, for which the interface changes shape as a consequence of deformations taking place throughout the material. In nature, these flows are typically gravity-driven rather than fluid-driven. Common examples of non-inertial bulk flow are creeping soil on hillslopes[30,73] (FIG. 2b), slumping of the continental shelf[97], viscous relaxation of volcanoes[98] or slowly flowing glaciers[99]. In these examples, the material itself can be considered to have enough cohesion and internal rigidity to behave as a solid on seasonal timescales, yet appears to flow slowly on geological timescales. Rapid bulk flows also occur when inertial forces propagate throughout the material. Examples include soil liquefaction[100], and fluidization in debris[42] and pyroclastic[101] flows (FIG. 1). In these systems, the volume of the particulate flow — and hence the location of the particle–fluid interface — is determined in part by shear-induced dilation and pore-pressure effects within the bulk[42,43,76].

These two types of mechanisms can, of course, both be present. One example is sedimentation, which can be thought of as the emergence of a boundary between the solid and the liquid phases. The interface is formed as the settling of particles is hindered by crowding, and the downward speed of the interface is determined by further consolidation of the bulk[102]. As expected for soft materials, sedimentation dynamics are strongly influenced by thermal effects[103,104] and inter-particle attraction and repulsion[104,105]. These dynamics are relevant for many geophysical flows, for example, turbidity currents: their upper boundary forms by sedimentation; however, this interface evolves under the influence of mixing and/or settling within the current (that is, bulk flow), as well as de-stabilizing fluid shear at the boundary (that is, interface-driven flow)[40,77–79] (FIG. 3). Fluid muds are a similar case: sedimentation occurs as attractive particles aggregate, but aggregates are resuspended by waves and currents[82]. Besides sedimentation, other examples of combined interfacial and bulk deformation may be found in landslides and glaciers, for which shear localization at the base of the flows produces an interface between the bulk flow and the underlying substrate (FIG. 2c). This lower boundary may be bedrock or an internal slip plane; in either case, shear-banding may occur at the interface, often due to large confining pressures and the associated effects of lubrication or pore pressure[74,106].

Soft-matter concepts in earth materials

As soft-matter physics has matured as a field over the past several decades, a number of central themes have developed[31,32]. Here, we highlight several that have the most relevance for geomorphology.

Rheology. The pioneering work of Ralph Alger Bagnold gave rise to important components of both soft-matter physics and geomorphology. Bagnold recognized that particulate geophysical flows span a gradient from granular to hydrodynamic control — what we would today call dense-granular flows to dilute suspensions — and sought a generalized rheology to connect the grain-inertia-dominated regime to the fluid-viscosity-dominated regime[2]. This class of materials is now referred to as granular suspensions[60], mixtures of fluids with athermal and non-attractive particles. Key insights of Bagnold's rheology are that dissipation via collisions depends on both particle concentration and shear rate (BOX 1). This work formed the foundation for Bagnold's approach to sediment transport in rivers[107,108] and also for early models of debris-flow rheology and associated dilatancy[109]; a kernel of it survives in the constitutive relations employed today to describe geophysical flows[76,95]. Bagnold's rheology was the seed for the so-called $\mu(I)$ rheology, a phenomenological constitutive relation between an effective friction (μ) and the dimensionless shear rate (I) that has recently been shown to unite granular and suspension rheology in a common framework[60,67] (BOX 1). Although the $\mu(I)$ rheology has been empirically successful and allowed for fruitful comparisons across a variety of systems, it is worth noting that the underlying equations are ill-posed for some regimes of parameter space[110], as is also the case for critical-state soil mechanics[111]. Resolving these issues is a matter of current research[112], which suggests that the inclusion of compressibility in the model can restore its well-posedness.

Cohesion
Component of shear strength that is independent of inter-particle friction (geotechnical) or the finite force required to separate two particles in contact (physics); our usage is compatible with both.

Shear localization
Deformation of a material is accommodated within a small region; one example is shear banding associated with a region 5–10 particles across, and another is shear transformation zones defined below.

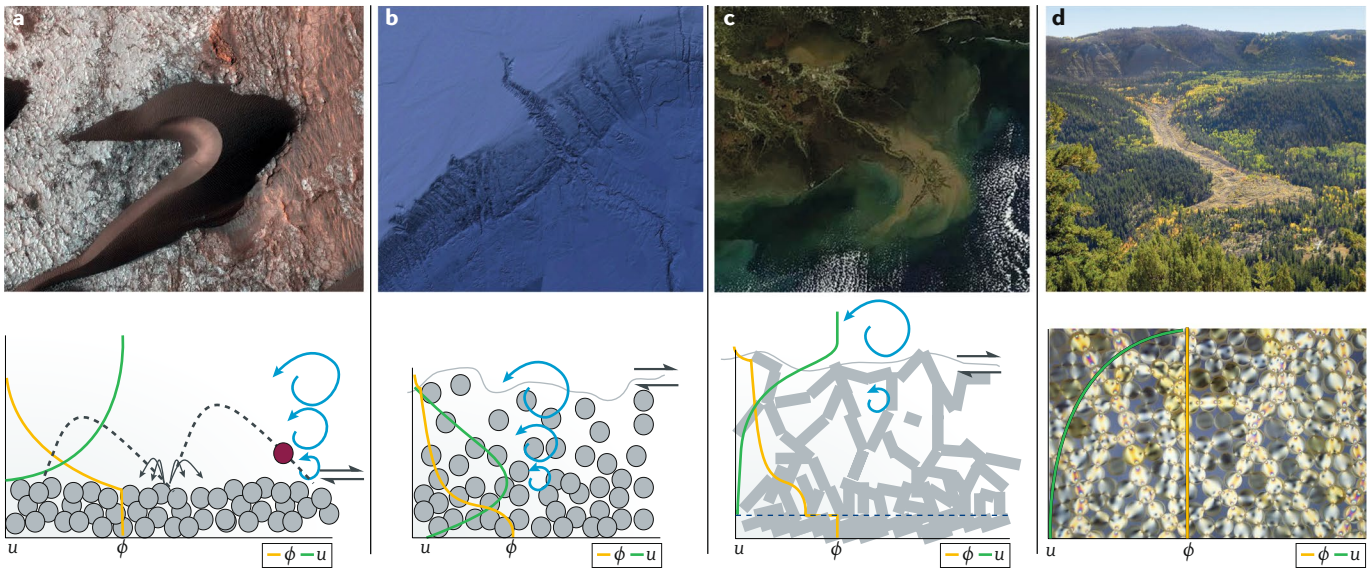

Fig. 3 | **Example landscape patterns and particle–fluid interactions of associated flows.** Particle or fluid velocity (u) and particle volume fraction (ϕ) are plotted schematically on linear axes. Blue swirls indicate where turbulence is relevant and opposing half arrows indicate fluid shear at an interface. **a** | Sand dune on Mars created by wind-driven sand transport. The dune is several hundred metres in width. Particle interactions are partially elastic (repulsive) collisions of grains with the bed (dashed lines show trajectories), which can cause other grains to splash up (black arrows). **b** | Submarine canyon and channel carved by turbidity currents. The entire channel is ~150 km long. Particles within the current interact via hydrodynamic repulsion and lubrication, forming a sheared, hindered settling interface (traced in grey); turbulence keeps grains suspended. **c** | Mud suspension emanating from the Mississippi Delta. The width of the end of the delta that sticks out is ~50 km. Some clay-rich suspensions form fluid muds by particle attraction; the mud is sheared from above (grey line). The dashed line marks the boundary with the irreversibly compacted mud substrate below. **d** | A creeping landslide or earthflow. The width of the flowing soil 'channel' is on order of tens of metres. Highly concentrated particles interact frictionally under gravity-driven, quasi-static shear. The lower part shows force chains, which become important for stress transmission. Colour intensity corresponds to force magnitude[273]. The photo in panel **a** is courtesy of NASA/JPL-Caltech/University of Arizona. The photo in panel **b** is courtesy of Data LDEO-Columbia, NSF, NOAA Data SIO, NOAA, U.S. Navy, NGA, GEBCO. The photo in panel **c** is courtesy of the NASA Worldview application (https://worldview.earthdata.nasa.gov), part of the NASA Earth Observing System Data and Information System (EOSDIS). The photo in panel **d** is courtesy of the Utah Geological Survey.

Earth materials that fall into the category of granular flows or suspensions include landslides[75,113], debris flows[42,114] and river sediment transport[16,93] (FIG. 1). All of these flows may be characterized by a viscoplastic rheology: below a critical shear rate or yield stress associated with inter-granular friction, they are solid-like; above yield, they exhibit shear-rate-dependent viscosity or friction. Two primary challenges for rheological descriptions of these particulate systems are to account for sub-yield creep, which is ubiquitous in granular materials[30,57,92,94,115–118], and how to correctly couple rheological models to their boundaries, via the correct boundary conditions. Nonlocal constitutive relations have been proposed that successfully explain the extension of above-yield flow into sub-yield regions for many flow configurations[119–122]. However, such models cannot account for phenomena such as purely sub-yield creep that occurs even in the absence of any flowing layer[94,117], slip near solid boundaries, the geometry of shear bands[66,123], the transition from inertial to creeping flow[124] or fluidization at distances far from disturbance[115,125]. For materials composed of colloidal (rather than granular) particles, additional classes of behaviour can arise from thermal effects or inter-particle attraction[56]; each of these classes may be mapped to earth materials in nature (BOX 1; FIG. 3).

Mohr–Coulomb failure
A solid mechanical failure criterion that determines the shear and normal stresses required to cause fracture in a frictional material.

Rigidity. The zeroth-order problem in geomorphology is to determine under what conditions material will move, and yet it remains particularly challenging[92]. Typical Mohr–Coulomb failure models do not appropriately describe the solid–liquid phase transition of geophysical flows, whether from entrainment of riverbed sediment by an impinging fluid[28] or the bulk liquefaction that creates landslides[14,42,43]. For example, geotechnical models for landslide failure consider soil to be a solid with a well-defined shear strength, above which it yields[126,127]. Attractive forces between particles (cohesion) effectively increase this shear strength, whereas an increase in pore pressure (due to water content) lowers shear strength by reducing the resisting normal stress[70,128]. The slow, sub-yield creeping motion of soil is considered to be a type of viscous flow that is modelled separately using simple constitutive equations[72,129]. In principle, the solid-state failure model and the sub-yield creeping 'flow' model are physically incompatible. In practice, these two models require site-specific calibrations and parameterizations that limit their predictive power[130].

Rigidity transitions of this type are central concepts in soft-matter physics[131], and it is possible to draw connections between the frictionless jamming transition[62] and frictional geophysical flows. For simplicity, here, we consider jamming to be a rapid increase in rigidity that

Fragile
A metastable state in which very small perturbations can lead to structural rearrangements and/or flow.

Shear transformation zones
(Also known as STZs). Small regions within an amorphous solid which undergo localized, plastic deformation due to an applied load.

Depinning
The phenomenon in which an interface within a rough potential-energy landscape becomes unstable and slips.

Excluded volume
Volume that a particle cannot occupy because another particle is already at that location.

is typically associated with an increase in volume fraction ϕ towards a critical value ϕ_c; unjamming is a corresponding decrease in rigidity. The nature of the jamming transition, however, is sensitive to particle contacts and interactions[132–134] and inter-particle friction[135,136], factors that are important for geophysically relevant properties such as dilatancy[137].

For example, granular materials may jam under shear as force networks are formed, but these jammed states may be fragile or robust, depending on the shear-stress magnitude[116,138] (FIG. 3). The jammed states can be responsible for arresting flowing materials[139]. The solid–liquid transition in geophysical flows is dependent on volume fraction[79,140], shear stress[42,76] and lubrication[113,141]; concepts from jamming should, therefore, be readily applicable to earth materials[14]. Yet, it is unclear whether Earth-surface materials actually jam. The pervasive sub-yield creep observed in granular heaps[30,117] and fluid-driven granular beds[94] occurs at volume fractions and stress values for which athermal materials would be expected to be jammed. Yield in these free-surface flows appears to exhibit the dynamics of a glass-to-liquid transition[30,117], for which frameworks such as shear transformation zones[57] and depinning[142–144] become relevant; we return to this below.

A related rigidity transition in dense suspensions is discontinuous shear thickening, which has been suggested to result from a stress-driven transition from lubricated to frictional granular contacts[145,146] or from interlocking asperities[133]. However, its causes and interpretation as a true phase transition have been the subject of much debate[147–150]. An additional rigidity transition that is relevant for geophysical materials is the sol–gel transition in attractive colloidal suspensions, in which percolated particle networks form, leading to the emergence of a yield stress. Long-range particle interactions allow this transition to occur even at very low ϕ (REFS[59,80]). These dynamics are thought to govern fluid-mud formation[81,82].

Excluded-volume effects and landscapes of valid states. A common feature of soft-matter systems is the presence of excluded-volume effects: a particle or molecule is excluded from accessing some position owing to the presence of a particle or molecule at a location overlapping that position. This property is particularly relevant to particulate systems[151], for which the cooperative effects of excluded volume lead to the presence of effective friction[152,153] and cohesion[154], even in the absence of either material friction or attractive forces. The relative importance of this effect can be determined from ϕ on its approach to ϕ_c (FIG. 1). Excluded-volume effects are at the heart of many of the jamming and rheological phenomena discussed in BOX 1.

Geophysical flows with particles packed closely enough for these effects to be relevant — that is, $\phi \rightarrow \phi_c$ — are common (FIG. 1). A consequence of volume exclusion is that, if creating a state would require two particles to overlap, then that state is inaccessible within a landscape of valid states, something analogous to a complex energy landscape for molecular systems[155]. (As the physics usage of the word 'landscape' will necessarily conflict with the geomorphological usage, we indicate all instances of the physics usage by calling it the 'landscape of valid states', where each valid state is a particular geological landscape.) Because granular materials are athermal and out of equilibrium, determining the correct constraints on their states is an open question and likely involves both positions (volume exclusion) and stresses (force and torque balance)[156]. Taking the analogy to energy landscapes, disordered packings exist in a high-dimensional landscape of valid states. Rearrangements into valid nearby states may be forbidden or favoured under some given driving (FIG. 4), and being trapped for long times in metastable states is a common occurrence. However, because Earth is constantly driven, the real landscape eventually finds an unstable manifold within the landscape of valid states and the dynamics occur along that unstable direction. Therefore, these complex landscapes of valid states contribute to the fragile and/or ageing nature of many soft materials, and can lead to interesting effects, such as metastability[157], intermittency[158], hysteresis[159], protocol-dependence[25] and the relaxation into limit cycles in which memories can be stored[160]. Each of these dynamics corresponds to different types of trajectories on the landscape of valid states.

Case studies

Fragile states. Earth landscapes are driven, out-of-equilibrium systems. Consider a mountain range: the horizontal convergence of tectonic plates leads to a piling up of rock to a critical angle, beyond which the wedge

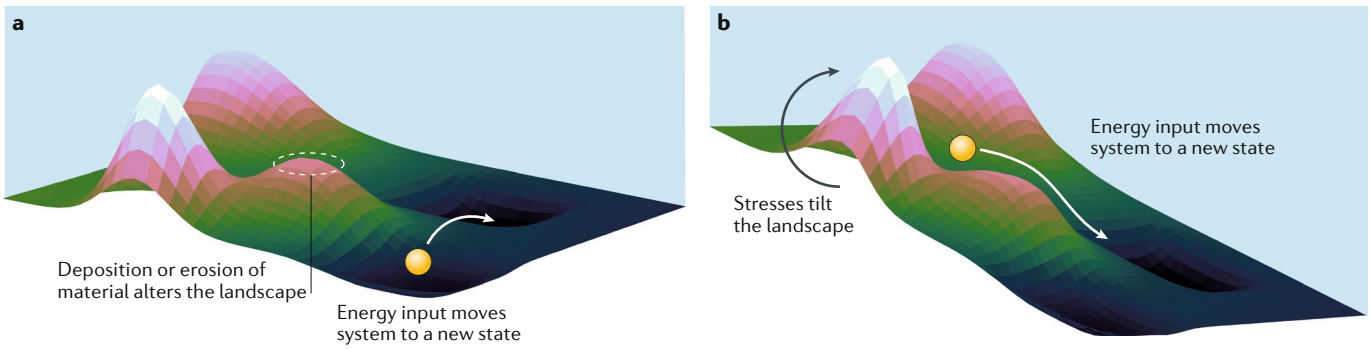

Fig. 4 | **The landscape of valid states (geological landscapes).** The spheres represent the current state of the system and must lie on the surface of this landscape of valid states. External forces can drive the system to find new states.

grows while maintaining a constant angle[161]. Locally, this growth is an effective topographic source term called uplift, which creates potential energy for transport. Erosion results as physical and chemical weathering break down rock into particulate material — eventually turning boulders into clays — which moves downhill by geophysical motions described above. Over geologic timescales, a steady state is reached in which erosion balances uplift on average[12]. Because the sediment-transport rate increases rapidly for stresses above the yield point, hillsides[30] and river channels[162] organize themselves, like a sandpile, to be in the vicinity of yield. A result of this self-organization is that mountain landscapes flicker back and forth across the yield transition, owing to environmental perturbations such as rainfall and floods, freeze–thaw cycles and earthquakes. Continental shelf environments are similarly self-organized: sediment sourced from rivers and delivered to the shelf edge piles up on the continental slope, where earthquakes and storms trigger dense (debris) flows and dilute particulate (turbidity) currents that relax the over-steepened slope[7]. Poorly understood fluid muds[81,82] are even more fragile, and their location in vulnerable estuaries and coastlines will make understanding their dynamics particularly important in a time of changing sea levels.

Thus, landscapes are driven to the fragile state — where dynamics such as sub-yield creep, ageing, hysteresis and failure occur. It is interesting that these behaviours, which are typically associated with glasses, occur in granular materials despite the irrelevance of thermal energy. This suggests that mechanical noise may play a role akin to thermal fluctuations[57,61,115,116,118]; we pick up this thread later.

Landscape patterns. In his seminal 1941 book[1], Bagnold laid out an approach for connecting the grain-scale physics of sand transport to the formation and evolution of wind-blown dunes. In the past two decades, a mature body of work has developed around testing and elaborating on his hypotheses. A key early result was the demonstration that the saturation length determines the length scale of dune formation[163]. The saturation length is the distance needed to achieve balance between grain inertia and wind strength[164]. This finding opened up sand dunes to laboratory exploration, because the density difference between water and air allows the creation of scaled-down dunes underwater[163,165]. Models that include simplified aerodynamics, avalanching and the saturation length were able to reproduce the pattern and scale of sand dunes observed in laboratory experiments[165] and the field[166–169]. Even the feedback mechanisms between vegetation growth and inhibition of sand transport have been encoded into models[170] that have been quantitatively confirmed with field data[171] (BOX 2).

Grain-scale sediment transport has also been connected to river-channel formation and associated landscape patterns. The simplest model for the cross-sectional shape of a river — that the riverbed surface is at the threshold of motion — has been quantitatively confirmed in the laboratory[172,173]. Remarkably, compilations of field data also show that the central tendency of natural rivers conforms to this prediction[162,174,175]. Alluvial fans are cones of sediment built by a migrating river channel; experiments[176,177] and field observations[178,179] have shown how the threshold of motion determines the overall shape of fan profiles (BOX 2). Experiments and field observations of drainage network patterns, and their temporal evolution, show surprisingly good agreement with an idealized theory for the growth of threshold channels in a Laplacian field[52,180]. This theory also reveals the connections of river network growth to a broader class of geophysical patterns that includes fracturing[181].

Unifying fluid-sheared sediment transport. Particulate transport in rivers is traditionally separated into two regimes. The first is bed-load transport, in which particles remain in close contact with the sediment bed as they move and are supported by it. The second is suspension, in which fluid-induced dispersion counteracts particle settling[90] (FIG. 2). In addition to these two regimes, wind-blown sand transport is distinguished from river transport by the larger significance of granular impacts on the entrainment of particles[1] (FIG. 3).

However, a new and rapidly developing understanding is emerging from explicit examination of granular dynamics that is leading to a unified description of fluid-driven particulate flows. Laboratory experiments in laminar[16,96] and transitionally turbulent[182] fluid flows have examined sediment transport by tracking particle motion from the interface to deep beneath, using refractive-index-matched scanning. The results show three distinct regimes at different depths in the sediment (FIG. 2a). The upper regime is a dilute granular suspension with low ϕ and large u that is dominated by hydrodynamic effects. At the base of the region, ϕ rapidly increases and u rapidly decreases at what may be considered the fluid–particle interface. The flowing layer of mobile grains below is the second regime, known as the bed-load layer. This region is characterized by approximately constant (and large) ϕ and u that decreases exponentially with depth; granular frictional effects dominate here. Below the bed-load layer, a kink in the velocity profile to a slower, second exponential decay marks the transition to the third, creep, regime (FIG. 1).

The entire range of bed-load to suspended-sediment transport, that is, the first and second regimes, follows $\mu(I)$ rheology[14,16]. Discrete element method (DEM) simulations driven by a statistically representative model of fluid turbulence suggest that $\mu(I)$ rheology may be extended to the turbulent-flow regime[93]. Such models have also demonstrated the importance of granular collisions and viscous dissipation in determining the momentum balance, and resultant transport rate, of the flowing granular layer. These effects may be accounted for by the introduction of a Stokes-like number[68,183], which, together with $\mu(I)$, provides a unified framework for describing sediment transport by wind and water. Some predictions emerging from these grain-scale models have been confirmed by field measurements of sediment transport in rivers[23,184] and sand dunes[41] (BOX 2).

Creep and the onset of flow. For almost a century, a simple Coulomb friction criterion has formed the basis for predicting the particle-entrainment threshold

by water[185] and wind[1] flows. More recent DEM simulations, introduced above, have revealed new insights: first, the importance of granular collision and viscous dissipation in determining the conditions for sustained transport[68,183] and second, the role of granular structure in modulating the local stability of the sediment bed[186]. Complementary laboratory flume experiments, spanning the laminar to turbulent and low-to-high Stokes number regimes, have confirmed the importance of these two factors[22,24,28,182,187]; they have also revealed the presence of creep below the onset of transport[92,94]. This creep was found to cause the sediment bed to harden under strain[24,94] and drive slow, granular segregation[188]. These dynamics are expected to produce hysteresis in the onset and cessation of transport, an effect that has been observed in natural rivers[23] (BOX 2).

Another phenomenon traditionally described with a Coulomb model is the failure and fluidization that arises at the initiation of landslides[126,127]. An important conceptual advance is the mapping to a creep–flow transition

Box 2 | **Geophysical field methods for soft landscapes**

Sediment transport: New geophysical methods make it possible to probe the mechanics and dynamics of fluid-driven sediment transport in field settings. The dispersion of radio-tagged cobbles in rivers[251] has been used to validate bed-load transport models[184] and smart rocks are being developed that can measure the forces of grain collisions[252]. Sediment-transport rates in rivers and dune fields have also been estimated from a wide range of techniques, such as impact plates[23], optical gates[41], and passive[253] and active[254] acoustics.

Flow fields: The data required to determine relevant weather conditions for wind-blown dunes[255], and the hydrology for river channels[256], are freely available for many locations around the world via databases maintained by various government agencies. This information provides the boundary conditions for flows impinging on sediment beds and allows estimation of the time-averaged fluid shear stresses to which landforms adjust[162]. More detailed measurements are needed to critically test sediment-transport models. Fluid velocity and turbulent (Reynolds) stress profiles are now routinely collected in rivers and atmospheric flows using acoustic and optical Doppler techniques[41,254,257]. Many of these methods are also deployed in the laboratory. For example, acoustic techniques are often applied to optically opaque particulate suspensions such as turbidity currents to image the internal structure of these flows[258].

Topography: The explosion of high-resolution, topographic field data has transformed the discipline of geomorphology. In particular, ground-based[259] and aerial lidar (light detection and ranging) topography are rendering high-fidelity elevation maps of terrestrial landscapes that facilitate stringent hypothesis testing. These datasets are rapidly expanding in number and global coverage, and many are freely available online[260]. Access to seafloor topographic data (bathymetry), collected from seismic surveys conducted by boat, is also growing quickly[261]. When coupled with mass conservation and some knowledge of boundary conditions, topography may be used to assess the rheological behaviour of earth materials over geologic time[30,73]. In fast-changing landscapes such as active landslides[197] and migrating sand dunes[171], repeat topographic surveys have been used to directly measure spatial patterns and rates of erosion and deposition. Moreover, expanding data coverage facilitates the exploration and discovery of fascinating new Earth-surface patterns.

Deformation: Geotechnical measurements of active landslides in the field are used to produce high-resolution maps of ground displacement that constrain the kinetics. Vertical velocity profiles in soil are often collected within boreholes; the profiles measure the angular displacements of a string of inclinometer sensors[262]. Slope movement is often driven by fluctuations in groundwater levels, so some studies also collect precipitation and water table measurements[199]. Vertical deformation and soil moisture profiles may alternatively be collected with time-domain reflectometry, an impedance technique[263]. Spatially extended data on surface-soil motion is also collected using global positioning system (GPS)[264] and interferometric synthetic aperture radar (InSAR)[197,265]; these data complement the depth-resolved, but spatially localized, deformation profiles from boreholes. InSAR was recently used to document, in stunning spatial and temporal resolution, the creep-to-landslide transition on a California mountain side[194]. These field measurements are often coupled with laboratory tests of soil mechanical properties, using samples extracted from the field[198]. Machine-learning algorithms have been applied to ground-displacement and associated environmental data for hillslopes, in hopes of enhancing the forecasting of landslides in a fully automated and cost-effective manner[266].

Seismology: A rapidly developing area is seismic geomorphology. The research capitalizes on decades of advances in seismology (motivated by earthquakes), and the wide distribution of seismic arrays, to determine the location and magnitude of sediment transport[267,268]. Passive seismic monitoring has been used to detect rigidity changes in soil preceding landslide failure[269] and to interpret flow dynamics[270]. The seismic noise resulting from transport in the field shares tantalizing similarities with acoustic emissions from failing materials in the laboratory[210,211,271]; this should be further explored. Finally, seismic geomorphology has also examined how landscapes respond to shear imposed by earthquakes[267].

Inverting flow deposits: Geophysical flows, such as landslides, debris flows and floods, are sporadic and unpredictable. The largest flows are rare, with recurrence intervals of up to thousands of years. Furthermore, some flows, such as turbidity currents in the deep sea, occur in places that are difficult to access. As a consequence, the magnitude, duration and mechanics of many important geophysical flows cannot be observed directly; rather, they must be inferred by 'inverting' the deposits left behind. Evidence for extreme shear-weakening in very large landslides has been produced by linking landslide deposits to their distant sources[195]. Similarly, the discovery that subaqueous debris flows are capable of hydroplaning was first inferred from determining the runout of blocks on the ocean bottom[141]. Other observed patterns include particle size and sorting patterns[184,188], damage and wear of particle surfaces[34], and the presence and scales of preserved bed topography, such as ripples and dunes[88]; all of these may be used to constrain the energy of the formative flow. Inverting deposits to estimate 'paleohydraulics' is rapidly gaining use in the study of planetary surfaces, where it is often the only tool available for constraining environmental conditions[9,10].

of both landslide failure and the onset of fluid-sheared sediment transport. Laminar-flow experiments for the onset of sediment transport[16], discussed above, show that transport occurs as creep below a critical viscous number $I_v \sim 10^{-5}$ (FIG. 1). In those experiments, creep is characterized by intermittent and localized particle rearrangements that are phenomenologically similar to shear-transformation zones in amorphous solids[57], as well as a departure from the expected $\mu(I)$ curve. At sufficiently low driving stresses, creep occurs throughout the sediment; above a critical stress, a flowing surface layer develops that is underlain by creeping grains.

Gravity-driven, heap-flow experiments have exhibited all of the same creep behaviours[117,189,190], and DEM simulations have found a creep–flow transition at a critical inertial number $I_i \sim 10^{-5}$ (REF.[30]) — in quantitative agreement with fluid-driven transport. The relation between strain rate and stress across the creep–flow transition in the simulations is consistent with a plastic depinning model proposed to describe yielding in glasses[30,61]. Simulations have also added random disturbances to grain motion that represent environmental disturbances in the field and found that these disturbances influenced the rate but not the form of creep[30,191]. Field measurements of creeping soil and fast landslides show approximate agreement with simulations, indicating that important components of the creep–landslide transition are controlled by granular friction[30]. Other field studies indicate that reduction of friction in accelerating landslides is common[192–194] (BOX 2). Such behaviour is likely granular in origin — it has been proposed, for example, that acoustic emissions from granular shear may help fluidize large landslides[195] or to trigger earthquakes[196] — but this link has not yet been demonstrated[33].

As an interesting aside, in a dilute surface layer of bed-load transport, the spatial patterning of mobile regions is consistent with a plastic depinning behaviour[143]. Whether this transition on the surface of a fluid-driven particle flow is related to the transition in the bulk of a gravity-driven heap flow is unknown; however, both involve disorder and cooperative particle motion. The case of a dilute bed-load layer moving over a (quasi-)static bed is fascinating for another reason: the landscape of valid states and the real (topographic) landscape are the same (FIG. 4). Particles move over and around a disordered array of potential wells and barriers that are created by other particles, but this landscape also evolves as particles are entrained from and deposited on the interface.

Outstanding problems

Athermal creep and the role of mechanical noise. The sudden collapse and liquefaction of apparently solid soil, to form landslides and debris flows, is perhaps the most dramatic illustration of the need to better understand and predict the solid–liquid transition in granular materials. The best-studied scenario is landsliding induced by rainfall. The addition of water to the soil enhances pore pressure; this effect has been presumed to drive the soil to yield[193,194,197–199]. Earthquakes are another common driver of liquefaction[200]; in this case, the mechanism typically invoked is shear-induced elevation of pore pressure[201]. The most well-developed continuum models for landslide failure are built on two tenets from critical-state soil mechanics[127]: the yield criterion is given by a Mohr–Coulomb law and pore-fluid pressure reduces contact forces by reducing the effective normal stress[42,202].

However, both these tenets have shortcomings. Some issues with the applicability of the Mohr–Coulomb law were discussed above in the context of rigidity transitions in general. Simulations have also shown that the Mohr–Coulomb criterion fails even in weakly disordered materials, for which the failure plane instead emerges from the coalescence of interacting damaged clusters[203] (FIG. 2c). As for the role of pore-fluid pressure, it has been proposed that lubrication, rather than pore pressure directly, may be the primary driver of liquefaction in geophysical flows[113]. This proposal has not yet been tested experimentally, perhaps due to measurement challenges that need to be overcome. If loss of rigidity arises from a frictional-to-lubrication transition, it would suggest, in those cases, that soil liquefaction is the 'mirror' process of discontinuous shear thickening[59,146]. In some cases, such as failure of muddy material underwater, lubrication may instead be localized at a basal slip surface, leading to hydroplaning[141,204,205].

Any description of the solid–liquid transition in amorphous materials must account for creep; yet, creep in athermal granular systems is a frontier topic in soft-matter physics. The major challenge when dealing with granular matter is that, unlike in molecular glasses, concepts of 'temperature' and 'energy landscape' (of valid states) are poorly defined[61]. Granular creep is generally understood to be a transient relaxation process that decays logarithmically with time[21], as particles settle into more stable configurations. However, earth materials creep indefinitely, presumably because of ceaseless mechanical disturbances. Besides increases in pore pressure (owing to rainfall) and shaking (caused by earthquakes), geologists have invoked the generation of pore volume by biophysical disturbances such as trees and animals[71,73,206] to explain the creep of soil below the apparent angle of repose. These disturbances that are internal to the soil — rather than imposed at the boundaries — bear a resemblance to melting due to thermal vibrations in glasses, but the applicability of thermal activation concepts to mechanical noise is currently an open question[61] (FIG. 4).

One proposed conceptualization of mechanical noise is as a stress that tilts the landscape of valid states (FIG. 4), allowing particles to access a previously forbidden configuration, typically through localized plastic rearrangements. In contrast to thermal systems, however, the landscape of valid states changes as particles rearrange[61,207]. Recent experiments and simulations have begun to explore the consequences of a range of disturbances on athermal creep. Acoustic driving[39,208] and vibrations[209] enhance microslip and creep rates in confined granular systems. Intriguingly, acoustic emissions from creeping[210] and also fast-flowing[38] grains have been observed, which are now being related to stability and vibrational modes[211]. This raises the tantalizing possibility of detecting precursor creep events on

Plastic
Refers to rearrangements of particles that occur during creep or yield, and are irreversible.

approach to failure using seismology in the field, though such applications are likely a long way off. Small stress modulations, imposed on a granular pack by an intruder, are able to induce a steady-state and effectively viscoelastic creep regime[118]. Heap-flow DEM simulations in a channel, in which the only imposed disturbance was the presence of walls, also exhibit steady-state creep that does not decline over time[30].

The upshot of these results is that, although no formal theory mapping thermal to mechanical noise exists, the emerging phenomenological picture of athermal creep is that of glassy dynamics[57,117,118]. In particular, (granular-friction-mediated) relaxation and (mechanically induced) rejuvenation drive persistent creep. Indeed, creeping motions observed within a thermally influenced heap flow of micrometre-scale grains[212] bear striking similarity to shear-localized rearrangements in a creeping heap flow of sand[117]. Formalizing these similarities and probing a wider variety of mechanical disturbances that are relevant to geophysical flows on land and undersea[42,79,101,204,205] are exciting challenges.

Ageing and hysteresis. Landscape patterns on Earth's surface are buffeted by a wide spectrum of forcings, from turbulent eddies to entire tectonic plates. At first blush, it is not obvious that steady-state landforms should exist at all. However, the evolution of landscapes such as rivers and hillslopes to critical or near-critical states acts to filter out a wide range of environmental forcings[162,213], allowing the application of averaged models for the driving stress.

Soft-matter effects such as ageing, hysteresis and multiple stable states, however, suggest that there are situations where evolution of the microstructure of the material must be taken into account. As a simple example, consider the consolidation of mud by dewatering. As clay particles sediment, they form aggregates[214] and colloidal gels[82] with a microstructure reminiscent of a house of cards (FIG. 3). Continued sedimentation induces an irreversible collapse under the hydrostatic burden[215], to produce a dense fabric of aligned clay particles with strongly enhanced rigidity[216]. Another example is the role of transient hydrodynamic forcing, such as the evaporation of suspensions that gives rise to colloidal films, cracks and the celebrated coffee-ring effect[217,218]. Particles may be bonded by van der Waals forces, and even sintered by capillary forces. Re-wetting does not restore the original suspension[219], meaning that a time-averaged description of water content would not predict the state of matter; that is, hysteresis occurs. Fluctuating environmental forces on Earth's surface activate a range of mechanical responses that, ultimately, control the rigidity of soil and sediment in ways that are only just beginning to be explored.

Active and activated matter. Active matter, in which particles move and/or exert forces, is now a firmly established research area in soft-matter physics[220]. Yet, only recently has it been explicitly shown that active matter can change the rheology and state transitions in glassy and granular materials[221–223]. For example, the presence of bacteria, even in modest concentrations, acts to suppress sedimentation of passive particles[224]. This phenomenon should be significant for muddy suspensions in bacteria-rich natural rivers and estuaries.

In Earth-surface materials more broadly, the presence of small populations of active agents is pervasive; witness the bioturbation of mud, soil and gravel riverbeds by innumerable organisms — from worms to salmon to wombats[225–228]. Plants not only affect sediment transport rates but they qualitatively change river[229] and dune[170,171] patterns. Geologists have awakened to the importance, and in some cases perhaps dominance, of biophysical processes in shaping Earth's landscapes. However, models developed to account for the effects of biota are not based on mechanics; there is typically no explicit consideration of forces. A major challenge is whether active-matter concepts can be extended to systems in which active particles (in this case, organisms) are significantly larger than the surrounding passive grains. Small-scale physics experiments suggest some immediate avenues for exploration. One connection could be to link root growth into grains[230,231] to the mechanical wedging of tree roots that dilates soil and breaks down rock[73,206]. Insights from fibre-reinforced granular materials[232,233] may help in thinking more mechanistically about root-reinforced hillslopes. Perhaps a more distant but more intriguing question: does pervasive bioactivation of soil simply speed up creep rates by tilting the landscape of valid states (FIG. 4)? Or does it produce a behaviour that is mechanically distinct from the granular creep that physicists have encountered thus far?

Rheology of heterogeneous soft matter. The rheology of geophysical flows is sensitive to particle-size distribution and solids content[83,234,235]. For instance, debris flows are slurries typically consisting of clay-sized to sand-sized particles and water, and are capable of entraining boulders. Increasing sand content has been shown to increase their yield stress[236], and can even change bulk rheology from shear thinning to shear thickening[237] (BOX 1). We speculate that the change to shear thickening is related to the shutting off of lubrication associated with discontinuous shear thickening; however, it may also be due to large particles breaking up cohesive contact networks of clays. In debris flows, even subtle changes in rheology strongly influence strain-rate localization and boundary shear, and can lead to segregation of phases, such as the formation of a front composed of large grains whose interactions are dominated by granular friction[238,239]. The chemical properties of fine particles, especially surface charge, also matter. Different clay types produce different suspension rheology that is dependent on salinity[240], presumably due to cohesion. All of these factors influence the conditions for failure of debris flows and the destructive potential associated with their runout. In the case of failure underwater, the initial rheology of the grain mixture determines the degree of mixing with the overlying water, and can even switch the failure mode from a gradually collapsing pile to a hydroplaning block[204,205].

These issues are at the forefront of soft-matter physics: what is the role of physical and chemical particle properties in the rheology and jamming of suspensions

and granular flows? The unifying framework of $\mu(I)$ rheology is appealing in its simplicity and recent work has demonstrated how it may be generalized to account for various complicating factors. These include non-Newtonian carrier fluids[241], thermal effects[242] and cohesion[243,244]. However, qualitative changes in flow behaviour may be induced by particle polydispersity and shape[245,246], surface roughness[133], repulsion[145], hydrogen bonding[134], attraction[80] and capillary forces[247]. All of these factors ultimately influence the microstructure of particle arrangements and explicit accounting for these changes in bulk continuum models is a challenge.

Conclusion

Landscapes are composed of, and formed by, flows of soft matter. By mapping the composition and dynamics of geophysical flows to recent advances in soft-matter physics, we hope to reveal the potential of the latter to help improve understanding of natural hazards and landscape evolution. In several cases of particulate–fluid flows examined here, this potential is already being realized. Soft-matter approaches may be extended to other earth materials. For example, solid rock[248] and ice[99] likely share much in common with amorphous solids such as glass — albeit with additional complexities arising from partial melting and recrystallization under high pressures — whereas fragmented ice has been shown to behave as a jammed granular material[249]. Examining geophysical problems — and their associated materials, geometries and boundary conditions — can also reveal new physics or challenge existing frameworks. We see particular promise in building connections from grain to landscape scales, through the consideration of rheology, statistical physics and athermal noise.

Published online: 09 October 2019

1. Bagnold, R. A. *The Physics of Blown Sand and Desert Dunes* (Methuen, 1941).
2. Bagnold, R. A. Experiments on a gravity-free dispersion of large solid spheres in a Newtonian fluid under shear. *Proc. R. Soc. Lond. A Math. Phys. Eng. Sci.* **225**, 49–63 (1954).
Pioneering experimental paper on the rheology of granular suspensions and their connection to geophysical flows.
3. Seminara, G. Fluvial sedimentary patterns. *Annu. Rev. Fluid Mech.* **42**, 43–66 (2010).
4. Charru, F., Andreotti, B. & Claudin, P. Sand ripples and dunes. *Annu. Rev. Fluid Mech.* **45**, 469–493 (2013).
5. Huppert, H. E. & Sparks, R. S. J. Extreme natural hazards: population growth, globalization and environmental change. *Philos. Trans. R. Soc. A* **364**, 1875–1888 (2006).
6. Syvitski, J. P., Vörösmarty, C. J., Kettner, A. J. & Green, P. Impact of humans on the flux of terrestrial sediment to the global coastal ocean. *Science* **308**, 376–380 (2005).
7. Canals, M. et al. Slope failure dynamics and impacts from seafloor and shallow sub-seafloor geophysical data: case studies from the COSTA project. *Mar. Geol.* **213**, 9–72 (2004).
8. Rebesco, M. & Camerlenghi, A. (eds) *Contourites* Vol. 60 (Elsevier, 2008).
9. Greeley, R. *Introduction to Planetary Geomorphology* (Cambridge Univ. Press, 2013).
10. Grotzinger, J. P., Hayes, A. G., Lamb, M. P. & McLennan, S. M. in *Comparative Climatology of Terrestrial Planets* (eds Mackwell, S. J., Simon-Miller, A. A., Harder, J. W. & Bullock, M. A.) 439–472 (Univ. Arizona Press, 2013).
11. [no authors listed] The science of scenery. *Nature* **121**, 309–311 (1928).
12. Anderson, R. S. & Anderson, S. P. *Geomorphology: The Mechanics and Chemistry of Landscapes* (Cambridge Univ. Press, 2010).
13. Dietrich, W. E. et al. in *Prediction in Geomorphology* Vol. 135 (eds Wilcock, P. R. & Iverson, R. M.) 103–132 (American Geophysical Union, 2013).
14. Houssais, M. & Jerolmack, D. J. Toward a unifying constitutive relation for sediment transport across environments. *Geomorphology* **277**, 251–264 (2017).
15. Kang, D. H., Yun, T. S., Lau, Y. M. & Wang, Y. H. DEM simulation on soil creep and associated evolution of pore characteristics. *Comput. Geotech.* **39**, 98–106 (2012).
16. Houssais, M., Ortiz, C. P., Durian, D. J. & Jerolmack, D. J. Rheology of sediment transported by a laminar flow. *Phys. Rev. E* **94**, 062609 (2016).
17. Vasisht, V. V., Dutta, S. K., Del Gado, E. & Blair, D. L. Rate dependence of elementary rearrangements and spatiotemporal correlations in the 3D flow of soft solids. *Phys. Rev. Lett.* **120**, 018001 (2018).
18. Ghosh, A. et al. Direct observation of percolation in the yielding transition of colloidal glasses. *Phys. Rev. Lett.* **118**, 148001 (2017).
19. Courtland, R. E. & Weeks, E. R. Direct visualization of ageing in colloidal glasses. *J. Phys. Condens. Matter* **15**, S359–S365 (2002).
20. Bonn, D., Tanase, S., Abou, B., Tanaka, H. & Meunier, J. Laponite: aging and shear rejuvenation of a colloidal glass. *Phys. Rev. Lett.* **89**, 015701 (2002).
21. Hartley, R. R. & Behringer, R. P. Logarithmic rate dependence of force networks in sheared granular materials. *Nature* **421**, 928–931 (2003).
22. Charru, F., Mouilleron, H. & Eiff, O. Erosion and deposition of particles on a bed sheared by a viscous flow. *J. Fluid Mech.* **519**, 55–80 (2004).
23. Turowski, J. M., Badoux, A. & Rickenmann, D. Start and end of bedload transport in gravel-bed streams. *Geophys. Res. Lett.* **38**, L04401 (2011).
24. Masteller, C. C. & Finnegan, N. J. Interplay between grain protrusion and sediment entrainment in an experimental flume. *J. Geophys. Res. Earth Surf.* **122**, 274–289 (2017).
25. Bililign, E. S., Kollmer, J. E. & Daniels, K. E. Protocol dependence and state variables in the force-moment ensemble. *Phys. Rev. Lett.* **122**, 038001 (2019).
26. Weeks, E. R., Crocker, J. C., Levitt, A. C., Schofield, A. & Weitz, D. A. Three-dimensional direct imaging of structural relaxation near the colloidal glass transition. *Science* **287**, 627–631 (2000).
27. Keys, A. S., Abate, A. R., Glotzer, S. C. & Durian, D. J. Measurement of growing dynamical length scales and prediction of the jamming transition in a granular material. *Nat. Phys.* **3**, 260–264 (2007).
28. Frey, P. & Church, M. Bedload: a granular phenomenon. *Earth Surf. Process. Landf.* **36**, 58–69 (2011).
29. Charbonneau, P., Kurchan, J., Parisi, G., Urbani, P. & Zamponi, F. Glass and jamming transitions: from exact results to finite-dimensional descriptions. *Annu. Rev. Condens. Matter Phys.* **8**, 265–288 (2017).
30. Ferdowsi, B., Ortiz, C. P. & Jerolmack, D. J. Glassy dynamics of landscape evolution. *Proc. Natl Acad. Sci. USA* **115**, 4827–4832 (2018).
31. Frenkel, D. Soft condensed matter. *Phys. A* **313**, 1–31 (2002).
Review article drawing on a statistical physics approach, with examples from colloidal physics.
32. Nagel, S. R. Experimental soft-matter science. *Rev. Mod. Phys.* **89**, 025002 (2017).
Survey of current open questions, drawn up during a workshop targeting the frontiers of the field.
33. Delannay, R., Valance, A., Mangeney, A., Roche, O. & Richard, P. Granular and particle-laden flows: from laboratory experiments to field observations. *J. Phys. D* **50**, 053001 (2017).
34. Novák-Szabó, T. et al. Universal characteristics of particle shape evolution by bed-load chipping. *Sci. Adv.* **4**, eaao4946 (2018).
35. Marone, C. Laboratory-derived friction laws and their application to seismic faulting. *Annu. Rev. Earth Planet. Sci.* **26**, 643–696 (1998).
36. Daniels, K. E. & Hayman, N. W. Force chains in seismogenic faults visualized with photoelastic granular shear experiments. *J. Geophys. Res.* **113**, B11411 (2008).
37. Hayman, N. W., Ducloué, L., Foco, K. L. & Daniels, K. E. Granular controls on periodicity of stick-slip events: kinematics and force-chains in an experimental fault. *Pure Appl. Geophys.* **168**, 2239–2257 (2011).
38. van der Elst, N. J., Brodsky, E. E., Le Bas, P.-Y. & Johnson, P. A. Auto-acoustic compaction in steady shear flows: experimental evidence for suppression of shear dilatancy by internal acoustic vibration. *J. Geophys. Res. Solid Earth* **117**, B09314 (2012).
39. Ferdowsi, B. et al. Acoustically induced slip in sheared granular layers: application to dynamic earthquake triggering. *Geophys. Res. Lett.* **42**, 9750–9757 (2015).
40. Parker, G., Garcia, M., Fukushima, Y. & Yu, W. Experiments on turbidity currents over an erodible bed. *J. Hydraul. Res.* **25**, 123–147 (1987).
41. Martin, R. L. & Kok, J. F. Wind-invariant saltation heights imply linear scaling of aeolian saltation flux with shear stress. *Sci. Adv.* **3**, e1602569 (2017).
42. Iverson, R. M., Reid, M. E. & LaHusen, R. G. Debris-flow mobilization from landslides. *Annu. Rev. Earth Planet. Sci.* **25**, 85–138 (1997).
43. Iverson, R. M. & Denlinger, R. P. Flow of variably fluidized granular masses across three-dimensional terrain: 1. Coulomb mixture theory. *J. Geophys. Res. Solid Earth* **106**, 537–552 (2001).
44. Furbish, D. J., Haff, P. K., Roseberry, J. C. & Schmeeckle, M. W. A probabilistic description of the bed load sediment flux: 1. Theory. *J. Geophys. Res. Earth Surf.* **117**, F03031 (2012).
Formulation of a formal statistical mechanics framework for sediment transport.
45. Furbish, D. J., Fathel, S. L., Schmeeckle, M. W., Jerolmack, D. J. & Schumer, R. The elements and richness of particle diffusion during sediment transport at small timescales. *Earth Surf. Process. Landf.* **42**, 214–237 (2017).
46. Einstein, H. A. *The Bed-Load Function for Sediment Transportation in Open Channel Flows* Vol. 1026 (US Dept. Agric., 1950).
47. Dodds, P. S. & Rothman, D. H. Scaling, universality, and geomorphology. *Annu. Rev. Earth Planet. Sci.* **28**, 571–610 (2000).
48. Schumer, R., Meerschaert, M. M. & Baeumer, B. Fractional advection-dispersion equations for modeling transport at the Earth surface. *J. Geophys. Res. Earth Surf.* **114**, F00A07 (2009).
49. Ancey, C., Bohorquez, P. & Heyman, J. Stochastic interpretation of the advection-diffusion equation and its relevance to bed load transport. *J. Geophys. Res. Earth Surf.* **120**, 2529–2551 (2015).
50. Rodríguez-Iturbe, I. & Rinaldo, A. *Fractal River Basins: Chance and Self-organization* (Cambridge Univ. Press, 2001).
51. Murray, A. B. et al. Geomorphology, complexity, and the emerging science of the Earth's surface. *Geomorphology* **103**, 496–505 (2009).
52. Devauchelle, O., Petroff, A. P., Seybold, H. F. & Rothman, D. H. Ramification of stream networks. *Proc. Natl Acad. Sci. USA* **109**, 20832–20836 (2012).
53. Goehring, L. Pattern formation in the geosciences. *Philos. Trans. R. Soc. A* **371**, 20120352 (2013).
Lead article for a special issue that summarizes the principles of non-equilibrium pattern formation, with many illustrative examples provided.

54. Paola, C., Straub, K., Mohrig, D. & Reinhardt, L. The "unreasonable effectiveness" of stratigraphic and geomorphic experiments. *Earth Sci. Rev.* **97**, 1–43 (2009).
55. Malverti, L., Lajeunesse, E. & Métivier, F. Small is beautiful: upscaling from microscale laminar to natural turbulent rivers. *J. Geophys. Res. Earth Surf.* **113**, F04004 (2008).
56. Chen, D. T., Wen, Q., Janmey, P. A., Crocker, J. C. & Yodh, A. G. Rheology of soft materials. *Annu. Rev. Condens. Matter Phys.* **1**, 301–322 (2010).
57. Falk, M. L. & Langer, J. S. Deformation and failure of amorphous, solidlike materials. *Annu. Rev. Condens. Matter Phys.* **2**, 353–373 (2011).
Review of the concepts and applicability of shear transformation zones.
58. Denn, M. M. & Morris, J. F. Rheology of non-Brownian suspensions. *Annu. Rev. Chem. Biomol. Eng.* **5**, 203–228 (2014).
59. Bonn, D., Denn, M. M., Berthier, L., Divoux, T. & Manneville, S. Yield stress materials in soft condensed matter. *Rev. Mod. Phys.* **89**, 035005 (2017).
A review of nonlinear behaviours spanning colloids, gels, emulsions, and suspensions.
60. Guazzelli, É. & Pouliquen, O. Rheology of dense granular suspensions. *J. Fluid Mech.* **852**, P1 (2018).
61. Nicolas, A., Ferrero, E. E., Martens, K. & Barrat, J.-L. Deformation and flow of amorphous solids: Insights from elastoplastic models. *Rev. Mod. Phys.* **90**, 045006 (2018).
62. Liu, A. J. & Nagel, S. R. The jamming transition and the marginally jammed solid. *Annu. Rev. Condens. Matter Phys.* **1**, 347–369 (2010).
A summary of the idealized framework by which disordered materials gain rigidity.
63. Gray, J. M. N. T. Particle segregation in dense granular flows. *Annu. Rev. Fluid Mech.* **50**, 407–433 (2018).
64. Amon, A. et al. Preface: focus on imaging methods in granular physics. *Rev. Sci. Instrum.* **88**, 051701 (2017).
65. de Gennes, P.-G. Soft matter. *Rev. Mod. Phys.* **64**, 645 (1992).
66. MiDi, G. On dense granular flows. *Eur. Phys. J. E* **14**, 341–365 (2004).
Introduces and justifies $\mu(I)$ rheology for describing dense granular flows.
67. Boyer, F., Guazzelli, É. & Pouliquen, O. Unifying suspension and granular rheology. *Phys. Rev. Lett.* **107**, 188301 (2011).
68. Pähtz, T. & Durán, O. Fluid forces or impacts: what governs the entrainment of soil particles in sediment transport mediated by a Newtonian fluid? *Phys. Rev. Fluids* **2**, 074303 (2017).
69. Dufek, J. The fluid mechanics of pyroclastic density currents. *Annu. Rev. Fluid Mech.* **48**, 459–485 (2016).
70. Bishop, A. W., Alpan, I., Blight, G. & Donald, I. in *Research Conference on Shear Strength of Cohesive Soils* (Am. Soc. Civ. Eng., 1960).
71. Culling, W. Soil creep and the development of hillside slopes. *J. Geol.* **71**, 127–161 (1963).
72. Garlanger, J. E. The consolidation of soils exhibiting creep under constant effective stress. *Géotechnique* **22**, 71–78 (1972).
73. Roering, J. J. Soil creep and convex-upward velocity profiles: theoretical and experimental investigation of disturbance-driven sediment transport on hillslopes. *Earth Surf. Process. Landf.* **29**, 1597–1612 (2004).
74. Okura, Y., Kitahara, H., Ochiai, H., Sammori, T. & Kawanami, A. Landslide fluidization process by flume experiments. *Eng. Geol.* **66**, 65–78 (2002).
75. Iverson, R. M. et al. Landslide mobility and hazards: implications of the 2014 Oso disaster. *Earth Planet. Sci. Lett.* **412**, 197–208 (2015).
76. Iverson, R. M., Logan, M., LaHusen, R. G. & Berti, M. The perfect debris flow? Aggregated results from 28 large-scale experiments. *J. Geophys. Res. Earth Surf.* **115**, F03005 (2010).
77. Kuenen, P. H. & Migliorini, C. I. Turbidity currents as a cause of graded bedding. *J. Geol.* **58**, 91–127 (1950).
78. Meiburg, E. & Kneller, B. Turbidity currents and their deposits. *Annu. Rev. Fluid Mech.* **42**, 135–156 (2010).
79. You, Y., Flemings, P. & Mohrig, D. Dynamics of dilative slope failure. *Geology* **40**, 663–666 (2012).
80. Colombo, J. & Del Gado, E. Stress localization, stiffening, and yielding in a model colloidal gel. *J. Rheol.* **58**, 1089–1116 (2014).
81. Winterwerp, J. C. On the flocculation and settling velocity of estuarine mud. *Cont. Shelf Res* **22**, 1339–1360 (2002).
82. McAnally, W. H. et al. Management of fluid mud in estuaries, bays, and lakes. I: Present state of understanding on character and behavior. *J. Hydraul. Eng.* **133**, 9–22 (2007).
83. Coussot, P. & Piau, J. M. On the behavior of fine mud suspensions. *Rheol. Acta* **33**, 175–184 (1994).
84. Cross, M. C. & Hohenberg, P. C. Pattern formation outside of equilibrium. *Rev. Mod. Phys.* **65**, 851–1112 (1993).
85. Fink, J. H. & Fletcher, R. C. Ropy pahoehoe: surface folding of a viscous fluid. *J. Volcanol. Geotherm. Res.* **4**, 151–170 (1978).
86. Griffiths, R. W. The dynamics of lava flows. *Annu. Rev. Fluid Mech.* **32**, 477–518 (2000).
87. Howard, A. D., Morton, J. B., Gad-El-Hak, M. & Pierce, D. B. Sand transport model of barchan dune equilibrium. *Sedimentology* **25**, 307–338 (1978).
88. Ayrton, H. The origin and growth of ripple-mark. *Proc. R. Soc. Lond.* **74**, 565–566 (1905).
89. Einstein, A. Die Ursache der Mäanderbildung der Flußläufe und des sogenannten Baerschen Gesetzes. *Naturwissenschaften* **14**, 223–224 (1926).
90. Raudkivi, A. J. *Loose Boundary Hydraulics* (CRC, 1998).
91. Lajeunesse, E., Malverti, L. & Charru, F. Bed load transport in turbulent flow at the grain scale: experiments and modeling. *J. Geophys. Res. Earth Surf.* **115**, F04001 (2010).
92. Houssais, M., Ortiz, C. P., Durian, D. J. & Jerolmack, D. J. Onset of sediment transport is a continuous transition driven by fluid shear and granular creep. *Nat. Commun.* **6**, 6527 (2015).
93. Maurin, R., Chauchat, J. & Frey, P. Dense granular flow rheology in turbulent bedload transport. *J. Fluid Mech.* **804**, 490–512 (2016).
94. Allen, B. & Kudrolli, A. Granular bed consolidation, creep, and armoring under subcritical fluid flow. *Phys. Rev. Fluids* **3**, 074305 (2018).
95. Capart, H. & Fraccarollo, L. Transport layer structure in intense bed-load. *Geophys. Res. Lett.* **38**, L20402 (2011).
96. Aussillous, P., Chauchat, J., Pailha, M., Médale, M. & Guazzelli, É. Investigation of the mobile granular layer in bedload transport by laminar shearing flows. *J. Fluid Mech.* **736**, 594–615 (2013).
97. Laughton, A. S. & Roberts, D. G. Morphology of the continental margin. *Philos. Trans. R. Soc. A* **290**, 75–85 (1978).
98. Byrne, P. K. et al. A sagging-spreading continuum of large volcano structure. *Geology* **41**, 339–342 (2013).
99. Goldsby, D. & Kohlstedt, D. Superplastic deformation of ice: experimental observations. *J. Geophys. Res. Solid Earth* **106**, 11017–11030 (2001).
100. Ishihara, K. Liquefaction and flow failure during earthquakes. *Géotechnique* **43**, 351–451 (1993).
101. Breard, E. C. et al. Coupling of turbulent and non-turbulent flow regimes within pyroclastic density currents. *Nat. Geosci.* **9**, 767–771 (2016).
102. Guazzelli, É. & Morris, J. F. *A Physical Introduction to Suspension Dynamics* Vol. 45 (Cambridge Univ. Press, 2011).
103. Ortiz, C. P., Riehn, R. & Daniels, K. E. Flow-driven formation of solid-like microsphere heaps. *Soft Matter* **9**, 543–549 (2013).
104. Brzinski, T. III & Durian, D. Observation of two branches in the hindered settling function at low Reynolds number. *Phys. Rev. Fluids* **3**, 124303 (2018).
105. Sutherland, B. R., Barrett, K. J. & Gingras, M. K. Clay settling in fresh and salt water. *Environ. Fluid Mech.* **15**, 147–160 (2015).
106. Clarke, G. K. Fast glacier flow: Ice streams, surging, and tidewater glaciers. *J. Geophys. Res. Solid Earth* **92**, 8835–8841 (1987).
107. Bagnold, R. A. The flow of cohesionless grains in fluids. *Philos. Trans. R. Soc.* **249**, 235–297 (1956).
108. Hunt, M., Zenit, R., Campbell, C. & Brennen, C. Revisiting the 1954 suspension experiments of RA Bagnold. *J. Fluid Mech.* **452**, 1–24 (2002).
109. Takahashi, T. Debris flow. *Annu. Rev. Fluid Mech.* **13**, 57–77 (1981).
110. Barker, T., Schaeffer, D. G., Bohórquez, P. & Gray, J. M. N. T. Well-posed and ill-posed behaviour of the $\mu(I)$-rheology for granular flow. *J. Fluid Mech.* **779**, 794–818 (2015).
111. Schaeffer, D. G. & Pitman, E. B. Ill-posedness in three-dimensional plastic flow. *Commun. Pure Appl. Math.* **41**, 879–890 (1988).
112. Barker, T., Schaeffer, D. G., Shearer, M. & Gray, J. M. N. T. Well-posed continuum equations for granular flow with compressibility and $\mu(I)$-rheology. *Proc. R. Soc. A* **473**, 20160846 (2017).
113. Ancey, C. Role of lubricated contacts in concentrated polydisperse suspensions. *J. Rheol.* **45**, 1421–1439 (2001).
114. Turnbull, B., Bowman, E. T. & McElwaine, J. N. Debris flows: experiments and modelling. *C. R. Phys.* **16**, 86–96 (2015).
115. Reddy, K., Forterre, Y. & Pouliquen, O. Evidence of mechanically activated processes in slow granular flows. *Phys. Rev. Lett.* **106**, 108301 (2011).
116. Bandi, M., Rivera, M., Krzakala, F. & Ecke, R. Fragility and hysteretic creep in frictional granular jamming. *Phys. Rev. E* **87**, 042205 (2013).
117. Amon, A., Bertoni, R. & Crassous, J. Experimental investigation of plastic deformations before a granular avalanche. *Phys. Rev. E* **87**, 012204 (2013).
Illuminates the structure and dynamics of athermal creep in a granular pile.
118. Pons, A., Darnige, T., Crassous, J., Clément, E. & Amon, A. Spatial repartition of local plastic processes in different creep regimes in a granular material. *EPL* **113**, 28001 (2016).
119. Pouliquen, O. & Forterre, Y. A non-local rheology for dense granular flows. *Philos. Trans. R. Soc. A* **367**, 5091–5107 (2009).
120. Kamrin, K. & Koval, G. Nonlocal constitutive relation for steady granular flow. *Phys. Rev. Lett.* **108**, 178301 (2012).
121. Bouzid, M. et al. Non-local rheology in dense granular flows – revisiting the concept of fluidity. *Eur. Phys. J. E* **38**, 125 (2015).
122. Tang, Z., Brzinski, T., Shearer, M. & Daniels, K. E. Nonlocal rheology of dense granular flow in annular shear experiments. *Soft Matter* **14**, 3040–3048 (2018).
123. Cheng, X. et al. Three-dimensional shear in granular flow. *Phys. Rev. Lett.* **96**, 038001 (2006).
124. Koval, G., Roux, J.-N., Corfdir, A. & Chevoir, F. Annular shear of cohesionless granular materials: From the inertial to quasistatic regime. *Phys. Rev. E* **79**, 021306 (2009).
125. Nichol, K., Zanin, A., Bastien, R., Wandersman, E. & van Hecke, M. Flow-induced agitations create a granular fluid. *Phys. Rev. Lett.* **104**, 078302 (2010).
126. Terzaghi, K. *Theoretical Soil Mechanics* (Wiley, 1943).
127. Schofield, A. & Wroth, P. *Critical State Soil Mechanics* Vol. 310 (McGraw-Hill, 1968).
128. Gan, J., Fredlund, D. & Rahardjo, H. Determination of the shear strength parameters of an unsaturated soil using the direct shear test. *Can. Geotech. J.* **25**, 500–510 (1988).
129. Savage, W. Z. & Chleborad, A. F. A model for creeping flow in landslides. *Environ. Eng. Geosci.* **19**, 333–338 (1982).
130. Zieher, T. et al. Sensitivity analysis and calibration of a dynamic physically based slope stability model. *Nat. Hazards Earth Syst. Sci.* **17**, 971–992 (2017).
131. Wyart, M. On the rigidity of amorphous solids. *Ann. Phys.* **30**, 1–96 (2005).
132. Basu, A. et al. Rheology of soft colloids across the onset of rigidity: scaling behavior, thermal, and non-thermal responses. *Soft Matter* **10**, 3027–3035 (2014).
133. Hsu, C.-P., Ramakrishna, S. N., Zanini, M., Spencer, N. D. & Isa, L. Roughness-dependent tribology effects on discontinuous shear thickening. *Proc. Natl Acad. Sci. USA* **115**, 5117–5122 (2018).
134. James, N. M., Hsu, C.-P., Spencer, N. D., Jaeger, H. M. & Isa, L. Tuning interparticle hydrogen bonding in shear-jamming suspensions: kinetic effects and consequences for tribology and rheology. *J. Phys. Chem. Lett.* **10**, 1663–1668 (2019).
135. Silbert, L. E. Jamming of frictional spheres and random loose packing. *Soft Matter* **6**, 2918–2924 (2010).
136. Henkes, S., van Hecke, M. & van Saarloos, W. Critical jamming of frictional grains in the generalized isostaticity picture. *EPL* **90**, 14003 (2010).
137. Schroeter, M. A local view on the role of friction and shape. *EPJ Web Conf.* **140**, 01008 (2017).
138. Bi, D., Zhang, J., Chakraborty, B. & Behringer, R. P. Jamming by shear. *Nature* **480**, 355–358 (2011).
Introduced the idea that rigidity can develop through a history of shear, rather than just the packing density.
139. Srivastava, I., Silbert, L. E., Grest, G. S. & Lechman, J. B. Flow-arrest transitions in frictional granular matter. *Phys. Rev. Lett.* **122**, 048003 (2019).
140. Rondon, L., Pouliquen, O. & Aussillous, P. Granular collapse in a fluid: role of the initial volume fraction. *Phys. Fluids* **23**, 073301 (2011).
141. Mohrig, D., Ellis, C., Parker, G., Whipple, K. X. & Hondzo, M. Hydroplaning of subaqueous debris flows. *Geol. Soc. Am. Bull.* **110**, 387–394 (1998).
142. Reichhardt, C. & Reichhardt, C. O. Depinning and nonequilibrium dynamic phases of particle assemblies driven over random and ordered substrates: a review. *Rep. Prog. Phys.* **80**, 026501 (2016).

143. Aussillous, P., Zou, Z., Guazzelli, É., Yan, L. & Wyart, M. Scale-free channeling patterns near the onset of erosion of sheared granular beds. *Proc. Natl Acad. Sci. USA* **113**, 11788–11793 (2016).
144. Ozawa, M., Berthier, L., Biroli, G., Rosso, A. & Tarjus, G. Random critical point separates brittle and ductile yielding transitions in amorphous materials. *Proc. Natl Acad. Sci. USA* **115**, 6656–6661 (2018).
145. Clavaud, C., Bérut, A., Metzger, B. & Forterre, Y. Revealing the frictional transition in shear-thickening suspensions. *Proc. Natl Acad. Sci. USA* **114**, 5147–5152 (2017).
146. Morris, J. F. Lubricated-to-frictional shear thickening scenario in dense suspensions. *Phys. Rev. Fluids* **3**, 110508 (2018).
147. Cheng, X., McCoy, J. H., Israelachvili, J. N. & Cohen, I. Imaging the microscopic structure of shear thinning and thickening colloidal suspensions. *Science* **333**, 1276–1279 (2011).
148. Mari, R., Seto, R., Morris, J. F. & Denn, M. M. Discontinuous shear thickening in Brownian suspensions by dynamic simulation. *Proc. Natl Acad. Sci. USA* **112**, 15326–15330 (2015).
149. Lin, N. Y. et al. Hydrodynamic and contact contributions to continuous shear thickening in colloidal suspensions. *Phys. Rev. Lett.* **115**, 228304 (2015).
150. Fall, A., Lemaître, A. & Ovarlez, G. Discontinuous shear thickening in cornstarch suspensions. *EPJ Web Conf.* **140**, 09001 (2017).
151. Caglioti, E., Loreto, V., Herrmann, H. J. & Nicodemi, M. A "tetris-like" model for the compaction of dry granular media. *Phys. Rev. Lett.* **79**, 1575–1578 (1997).
152. Lespiat, R., Cohen-Addad, S. & Hoehler, R. Jamming and flow of random-close-packed spherical bubbles: an analogy with granular materials. *Phys. Rev. Lett.* **106**, 148302 (2011).
153. Peyneau, P.-E. & Roux, J.-N. Frictionless bead packs have macroscopic friction, but no dilatancy. *Phys. Rev. E* **78**, 011307 (2008).
154. Gravish, N., Franklin, S., Hu, D. & Goldman, D. Entangled granular media. *Phys. Rev. Lett.* **108**, 208001 (2012).
155. Wales, D. J. *Energy Landscapes: Applications to Clusters, Biomolecules and Glasses* (Cambridge Univ. Press, 2003).
156. Bi, D., Henkes, S., Daniels, K. & Chakraborty, B. The statistical physics of athermal materials. *Annu. Rev. Condens. Matter Phys.* **6**, 63–83 (2015).
157. Iikawa, N., Bandi, M. & Katsuragi, H. Sensitivity of granular force chain orientation to disorder-induced metastable relaxation. *Phys. Rev. Lett.* **116**, 128001 (2016).
158. Nasuno, S., Kudrolli, A., Bak, A. & Gollub, J. P. Time-resolved studies of stick-slip friction in sheared granular layers. *Phys. Rev. E* **58**, 2161–2171 (1998).
159. DeGiuli, E. & Wyart, M. Friction law and hysteresis in granular materials. *Proc. Natl Acad. Sci. USA* **114**, 9284–9289 (2017).
160. Keim, N. C., Paulsen, J., Zeravcic, Z., Sastry, S. & Nagel, S. R. Memory formation in matter. *Rev. Mod. Phys.* **91**, 035002 (2018).
161. Davis, D., Suppe, J. & Dahlen, F. Mechanics of fold-and-thrust belts and accretionary wedges. *J. Geophys. Res. Solid Earth* **88**, 1153–1172 (1983).
162. Phillips, C. B. & Jerolmack, D. J. Self-organization of river channels as a critical filter on climate signals. *Science* **352**, 694–697 (2016).
163. Hersen, P., Douady, S. & Andreotti, B. Relevant length scale of barchan dunes. *Phys. Rev. Lett.* **89**, 264301 (2002).
164. Andreotti, B., Claudin, P. & Pouliquen, O. Measurements of the aeolian sand transport saturation length. *Geomorphology* **123**, 343–348 (2010).
165. Reffet, E., Courrech du Pont, S., Hersen, P. & Douady, S. Formation and stability of transverse and longitudinal sand dunes. *Geology* **38**, 491–494 (2010).
166. Hersen, P. et al. Corridors of barchan dunes: stability and size selection. *Phys. Rev. E* **69**, 011304 (2004).
167. Schwämmle, V. & Herrmann, H. J. A model of barchan dunes including lateral shear stress. *Eur. Phys. J. E* **16**, 57–65 (2005).
168. Ping, L., Narteau, C., Dong, Z., Zhang, Z. & Du Pont, S. C. Emergence of oblique dunes in a landscape-scale experiment. *Nat. Geosci.* **7**, 99–103 (2014).
169. Zhang, D., Narteau, C. & Rozier, O. Morphodynamics of barchan and transverse dunes using a cellular automaton model. *J. Geophys. Res. Earth Surf.* **115**, F03041 (2010).
170. Durán, O. & Herrmann, H. J. Vegetation against dune mobility. *Phys. Rev. Lett.* **97**, 188001 (2006).
171. Reitz, M. D., Jerolmack, D. J., Ewing, R. C. & Martin, R. L. Barchan-parabolic dune pattern transition from vegetation stability threshold. *Geophys. Res. Lett.* **37**, L19402 (2010).
172. Seizilles, G., Devauchelle, O., Lajeunesse, E. & Métivier, F. Width of laminar laboratory rivers. *Phys. Rev. E* **87**, 052204 (2013).
173. Reitz, M. D. et al. Diffusive evolution of experimental braided rivers. *Phys. Rev. E* **89**, 052809 (2014).
174. Métivier, F., Lajeunesse, E. & Devauchelle, O. Laboratory rivers: Lacey's law, threshold theory, and channel stability. *Earth Surf. Dyn.* **5**, 187–198 (2017).
175. Dunne, K. B. & Jerolmack, D. J. Evidence of, and a proposed explanation for, bimodal transport states in alluvial rivers. *Earth Surf. Dyn.* **6**, 583–594 (2018).
176. Reitz, M. D. & Jerolmack, D. J. Experimental alluvial fan evolution: Channel dynamics, slope controls, and shoreline growth. *J. Geophys. Res. Earth Surf.* **117**, F02021 (2012).
177. Delorme, P., Devauchelle, O., Barrier, L. & Métivier, F. Growth and shape of a laboratory alluvial fan. *Phys. Rev. E* **98**, 012907 (2018).
178. Parker, G. et al. Alluvial fans formed by channelized fluvial and sheet flow. II: application. *J. Hydraul. Eng.* **124**, 996–1004 (1998).
179. Miller, K. L., Reitz, M. D. & Jerolmack, D. J. Generalized sorting profile of alluvial fans. *Geophys. Res. Lett.* **41**, 7191–7199 (2014).
180. Berhanu, M., Petroff, A., Devauchelle, O., Kudrolli, A. & Rothman, D. H. Shape and dynamics of seepage erosion in a horizontal granular bed. *Phys. Rev. E* **86**, 041304 (2012).
181. Devauchelle, O. et al. Laplacian networks: growth, local symmetry, and shape optimization. *Phys. Rev. E* **95**, 033113 (2017).
182. Allen, B. & Kudrolli, A. Depth resolved granular transport driven by shearing fluid flow. *Phys. Rev. Fluids* **2**, 024304 (2017).
183. Durán, O., Andreotti, B. & Claudin, P. Numerical simulation of turbulent sediment transport, from bed load to saltation. *Phys. Fluids* **24**, 103306 (2012).
184. Phillips, C. B. & Jerolmack, D. J. Dynamics and mechanics of bed-load tracer particles. *Earth Surf. Dyn.* **2**, 513–530 (2014).
185. Shields, A. *Anwendung der aehnlichkeitsmechanik und der turbulenzforschung auf die geschiebebewegung*. Thesis, Technical Univ. Berlin (1936).
186. Clark, A. H., Shattuck, M. D., Ouellette, N. T. & O'Hern, C. S. Role of grain dynamics in determining the onset of sediment transport. *Phys. Rev. Fluids* **2**, 034305 (2017).
187. Lee, D. B. & Jerolmack, D. Determining the scales of collective entrainment in collision-driven bed load. *Earth Surf. Dyn.* **6**, 1089–1099 (2018).
188. Ferdowsi, B., Ortiz, C. P., Houssais, M. & Jerolmack, D. J. River-bed armouring as a granular segregation phenomenon. *Nat. Commun.* **8**, 1363 (2017).
189. Komatsu, T. S., Inagaki, S., Nakagawa, N. & Nasuno, S. Creep motion in a granular pile exhibiting steady surface flow. *Phys. Rev. Lett.* **86**, 1757–1760 (2001).
190. Crassous, J., Metayer, J.-F., Richard, P. & Laroche, C. Experimental study of a creeping granular flow at very low velocity. *J. Stat. Mech. Theory Exp.* **2008**, P03009 (2008).
191. Ben-Dror, E. & Goren, L. Controls over sediment flux along soil-mantled hillslopes: Insights from granular dynamics simulations. *J. Geophys. Res. Earth Surf.* **123**, 924–944 (2018).
192. Lucas, A., Mangeney, A. & Ampuero, J. P. Frictional velocity-weakening in landslides on earth and on other planetary bodies. *Nat. Commun.* **5**, 3417 (2014).
193. Handwerger, A. L., Rempel, A. W., Skarbek, R. M., Roering, J. J. & Hilley, G. E. Rate-weakening friction characterizes both slow sliding and catastrophic failure of landslides. *Proc. Natl Acad. Sci. USA* **113**, 10281–10286 (2016).
194. Handwerger, A. L., Huang, M.-H., Fielding, E. J., Booth, A. M. & Bürgmann, R. A shift from drought to extreme rainfall drives a stable landslide to catastrophic failure. *Sci. Rep.* **9**, 1569 (2019).
195. Melosh, H. The physics of very large landslides. *Acta Mechanica* **64**, 89–99 (1986).
196. Brodsky, E. E. & van der Elst, N. J. The uses of dynamic earthquake triggering. *Annu. Rev. Earth Planet. Sci.* **42**, 317–339 (2014).
197. Roering, J. J., Stimely, L. L., Mackey, B. H. & Schmidt, D. A. Using DInSAR, airborne LiDAR, and archival air photos to quantify landsliding and sediment transport. *Geophys. Res. Lett.* **36**, L19402 (2009).
198. Di Maio, C., Scaringi, G., Vassallo, R., Rizzo, E. & Perrone, A. in *Landslides and Engineered Slopes. Experience, Theory and Practice* Ch. 85 (eds Aversa, S., Cascini, L., Picarelli, L. & Scavia, C.) 813–820 (CRC, 2016).
199. Lollino, P., Giordan, D. & Allasia, P. Assessment of the behavior of an active earth-slide by means of calibration between numerical analysis and field monitoring. *Bull. Eng. Geol. Environ.* **76**, 421–435 (2017).
200. Meunier, P., Hovius, N. & Haines, J. A. Topographic site effects and the location of earthquake induced landslides. *Earth Planet. Sci. Lett.* **275**, 221–232 (2008).
201. Sassa, K., Fukuoka, H., Scarascia-Mugnozza, G. & Evans, S. Earthquake-induced-landslides: distribution, motion and mechanisms. *Soils Found.* **36**, 53–64 (1996).
202. Iverson, R. M. & George, D. L. A depth-averaged debris-flow model that includes the effects of evolving dilatancy. I. Physical basis. *Proc. R. Soc. A* **470**, 20130819 (2014).
203. Dansereau, V., Démery, V., Berthier, E., Weiss, J. & Ponson, L. Collective damage growth controls fault orientation in quasibrittle compressive failure. *Phys. Rev. Lett.* **122**, 085501 (2019).
204. Mohrig, D., Elverhøi, A. & Parker, G. Experiments on the relative mobility of muddy subaqueous and subaerial debris flows, and their capacity to remobilize antecedent deposits. *Mar. Geol.* **154**, 117–129 (1999).
205. Ilstad, T., Elverhøi, A., Issler, D. & Marr, J. G. Subaqueous debris flow behaviour and its dependence on the sand/clay ratio: a laboratory study using particle tracking. *Mar. Geol.* **213**, 415–438 (2004).
206. Roering, J. J. How well can hillslope evolution models explain topography? Simulating soil transport and production with high-resolution topographic data. *Geol. Soc. Am. Bull.* **120**, 1248–1262 (2008).
207. Agoritsas, E., Bertin, E., Martens, K. & Barrat, J.-L. On the relevance of disorder in athermal amorphous materials under shear. *Eur. Phys. J. E* **38**, 71 (2015).
208. Johnson, P. A., Savage, H., Knuth, M., Gomberg, J. & Marone, C. Effects of acoustic waves on stick–slip in granular media and implications for earthquakes. *Nature* **451**, 57–60 (2008).
209. Griffa, M. et al. Vibration-induced slip in sheared granular layers and the micromechanics of dynamic earthquake triggering. *EPL* **96**, 14001 (2011).
210. Johnson, P. et al. Acoustic emission and microslip precursors to stick-slip failure in sheared granular material. *Geophys. Res. Lett.* **40**, 5627–5631 (2013).
211. Brzinski, T. A. III & Daniels, K. E. Sounds of failure: passive acoustic measurements of excited vibrational modes. *Phys. Rev. Lett.* **120**, 218003 (2018).
212. Bérut, A., Pouliquen, O. & Forterre, Y. Avalanches of Brownian granular suspensions. Preprint at *arXiv* https://arxiv.org/abs/1908.10762 (2019).
Shows how thermal fluctuations influence creep and fluidization.
213. Jerolmack, D. J. & Paola, C. Shredding of environmental signals by sediment transport. *Geophys. Res. Lett.* **37**, L19401 (2010).
214. Allain, C., Cloitre, M. & Wafra, M. Aggregation and sedimentation in colloidal suspensions. *Phys. Rev. Lett.* **74**, 1478–1481 (1995).
215. Barden, L., McGown, A. & Collins, K. The collapse mechanism in partly saturated soil. *Eng. Geol.* **7**, 49–60 (1973).
216. Delage, P. & Lefebvre, G. Study of the structure of a sensitive Champlain clay and of its evolution during consolidation. *Can. Geotech. J.* **21**, 21–35 (1984).
217. Deegan, R. D. et al. Capillary flow as the cause of ring stains from dried liquid drops. *Nature* **389**, 827–829 (1997).
218. Deegan, R. D. Pattern formation in drying drops. *Phys. Rev. E* **61**, 475–485 (2000).
219. Goehring, L., Conroy, R., Akhter, A., Clegg, W. J. & Routh, A. F. Evolution of mud-crack patterns during repeated drying cycles. *Soft Matter* **6**, 3562–3567 (2010).
220. Marchetti, M. C. et al. Hydrodynamics of soft active matter. *Rev. Mod. Phys.* **85**, 1143–1189 (2013).
221. Berthier, L., Flenner, E. & Szamel, G. How active forces influence nonequilibrium glass transitions. *New J. Phys.* **19**, 125006 (2017).
222. Junot, G., Briand, G., Ledesma-Alonso, R. & Dauchot, O. Active versus passive hard disks against a membrane: mechanical pressure and instability. *Phys. Rev. Lett.* **119**, 028002 (2017).
223. Saintillan, D. Rheology of active fluids. *Annu. Rev. Fluid Mech.* **50**, 563–592 (2018).
224. Singh, J., Patteson, A. E., Purohit, P. K. & Arratia, P. E. Sedimentation and diffusion of passive particles in suspensions of swimming Escherichia coli. Preprint at *arXiv* https://arxiv.org/abs/1710.04068 (2017).

225. Butler, D. R. *Zoogeomorphology: Animals as Geomorphic Agents* (Cambridge Univ. Press, 1995).
226. Hassan, M. A. et al. Salmon-driven bed load transport and bed morphology in mountain streams. *Geophys. Res. Lett.* **35**, L04405 (2008).
227. Wilkinson, M. T., Richards, P. J. & Humphreys, G. S. Breaking ground: pedological, geological, and ecological implications of soil bioturbation. *Earth Sci. Rev.* **97**, 257–272 (2009).
228. Reinhardt, L., Jerolmack, D., Cardinale, B. J., Vanacker, V. & Wright, J. Dynamic interactions of life and its landscape: feedbacks at the interface of geomorphology and ecology. *Earth Surf. Process. Landf.* **35**, 78–101 (2010).
229. Tal, M. & Paola, C. Dynamic single-thread channels maintained by the interaction of flow and vegetation. *Geology* **35**, 347–350 (2007).
230. Kolb, E., Hartmann, C. & Genet, P. Radial force development during root growth measured by photoelasticity. *Plant Soil* **360**, 19–35 (2012).
231. Wendell, D. M., Luginbuhl, K., Guerrero, J. & Hosoi, A. E. Experimental investigation of plant root growth through granular substrates. *Exp. Mech.* **52**, 945–949 (2012).
232. Diambra, A., Ibraim, E., Muir Wood, D. & Russell, A. Fibre reinforced sands: Experiments and modelling. *Geotext. Geomembr.* **28**, 238–250 (2010).
233. Dos Santos, A. S., Consoli, N. & Baudet, B. The mechanics of fibre-reinforced sand. *Géotechnique* **60**, 791–799 (2010).
234. Major, J. J. & Pierson, T. C. Debris flow rheology: experimental analysis of fine-grained slurries. *Water Resour. Res.* **28**, 841–857 (1992).
235. Coussot, P. & Meunier, M. Recognition, classification and mechanical description of debris flows. *Earth Sci. Rev.* **40**, 209–227 (1996).
236. Scotto di Santolo, A., Pellegrino, A. M. & Evangelista, A. Experimental study on the rheological behaviour of debris flow. *Nat. Hazards Earth Syst. Sci.* **10**, 2507–2514 (2010).
237. Bardou, E., Boivin, P. & Pfeifer, H.-R. Properties of debris flow deposits and source materials compared: implications for debris flow characterization. *Sedimentology* **54**, 469–480 (2007).
238. Parsons, J. D., Whipple, K. X. & Simoni, A. Experimental study of the grain-flow, fluid-mud transition in debris flows. *J. Geol.* **109**, 427–447 (2001).
239. Leonardi, A. et al. Granular-front formation in free-surface flow of concentrated suspensions. *Phys. Rev. E* **92**, 052204 (2015).
240. Jeong, S. W., Locat, J., Leroueil, S. & Malet, J.-P. Rheological properties of fine-grained sediment: the roles of texture and mineralogy. *Can. Geotech. J.* **47**, 1085–1100 (2010).
241. Dagois-Bohy, S., Hormozi, S., Guazzelli, É. & Pouliquen, O. Rheology of dense suspensions of non-colloidal spheres in yield-stress fluids. *J. Fluid Mech.* **776**, R2 (2015).
242. Wang, M. & Brady, J. F. Constant stress and pressure rheology of colloidal suspensions. *Phys. Rev. Lett.* **115**, 158301 (2015).
243. Berger, N., Azéma, E., Douce, J.-F. & Radjai, F. Scaling behaviour of cohesive granular flows. *EPL* **112**, 64004 (2016).
244. Roy, S., Luding, S. & Weinhart, T. A general(ized) local rheology for wet granular materials. *New J. Phys.* **19**, 043014 (2017).
245. Nguyen, D.-H., Azéma, E., Sornay, P. & Radjai, F. Effects of shape and size polydispersity on strength properties of granular materials. *Phys. Rev. E* **91**, 032203 (2015).
246. Pednekar, S., Chun, J. & Morris, J. F. Bidisperse and polydisperse suspension rheology at large solid fraction. *J. Rheol.* **62**, 513–526 (2018).
247. Koos, E. & Willenbacher, N. Capillary forces in suspension rheology. *Science* **331**, 897–900 (2011).
248. Li, Q., Tullis, T. E., Goldsby, D. & Carpick, R. W. Frictional ageing from interfacial bonding and the origins of rate and state friction. *Nature* **480**, 233–236 (2011).
249. Burton, J. C., Amundson, J. M., Cassotto, R., Kuo, C.-C. & Dennin, M. Quantifying flow and stress in ice mélange, the world's largest granular material. *Proc. Natl Acad. Sci. USA* **115**, 5105–5110 (2018).
250. Lin, J. & Wyart, M. Microscopic processes controlling the Herschel–Bulkley exponent. *Phys. Rev. E* **97**, 012603 (2018).
251. Hassan, M. A. & Roy, A. G. in *Tools in Fluvial Geomorphology* Ch. 14 (eds Kondolf, G. M. & Piégay, H.) 306–323 (Wiley, 2016).
252. Underwood, E. Geomorphology: how to build a smarter rock. *Science* **338**, 1412–1413 (2012).
253. Geay, T. et al. Passive acoustic monitoring of bed load discharge in a large gravel bed river. *J. Geophys. Res. Earth Surf.* **122**, 528–545 (2017).
254. Church, M., Biron, P. & Roy, A. *Gravel Bed Rivers: Processes, Tools, Environments* (Wiley, 2012).
255. Horel, J. et al. Mesowest: Cooperative mesonets in the western United States. *Bull. Am. Meteorol. Soc.* **83**, 211–226 (2002).
256. Lins, H. F. USGS hydro-climatic data network 2009 (HCDN-2009). US Geological Survey fact sheet 2012-3047 (USGS, 2012).
257. de Arruda Moreira, G. et al. Study of the planetary boundary layer by microwave radiometer, elastic lidar and Doppler lidar estimations in Southern Iberian Peninsula. *Atmos. Res.* **213**, 185–195 (2018).
258. Perillo, M. M., Minton, B., Buttles, J. & Mohrig, D. Acoustic imaging of experimental subaqueous sediment-laden flows and their deposits. *J. Sediment. Res.* **85**, 1–5 (2015).
259. Telling, J., Lyda, A., Hartzell, P. & Glennie, C. Review of Earth science research using terrestrial laser scanning. *Earth Sci. Rev.* **169**, 35–68 (2017).
260. Krishnan, S. et al. in *Proc. 2nd Int. Conf. Comput. Geospat. Res. Appl*. 7 (ACM, 2011).
261. John, M. D., Campbell, K. J. & Devine, C. A. in *Offshore Technol. Conf*. (OTC, 2018).
262. Yufei, G. & Bing, H. Deformation mechanism and trend research on a creep landslide in Sichuan Province of China. *Electron. J. Geotech. Eng.* **17**, 3415–3428 (2012).
263. Lin, C.-P., Tang, S.-H., Lin, W.-C. & Chung, C.-C. Quantification of cable deformation with time domain reflectometry — implications to landslide monitoring. *J. Geotech. Geoenviron. Eng.* **135**, 143–152 (2009).
264. Wang, G. GPS landslide monitoring: single base vs. network solutions – a case study based on the Puerto Rico and Virgin Islands permanent GPS network. *J. Geod. Sci.* **1**, 191–203 (2011).
265. Zaugg, E. C., Bradley, J. P., Lee, H. & Cao, N. in *2016 IEEE Radar Conf. Proc.* (IEEE, 2016).
266. Tordesillas, A., Zhou, Z. & Batterham, R. A data-driven complex systems approach to early prediction of landslides. *Mech. Res. Commun.* **92**, 137–141 (2018).
267. Burtin, A., Hovius, N. & Turowski, J. M. Seismic monitoring of torrential and fluvial processes. *Earth Surf. Dyn.* **4**, 285–307 (2016).
268. Roth, D. L. et al. Bed load sediment transport inferred from seismic signals near a river. *J. Geophys. Res. Earth Surf.* **121**, 725–747 (2016).
269. Mainsant, G. et al. Ambient seismic noise monitoring of a clay landslide: toward failure prediction. *J. Geophys. Res. Earth Surf.* **117**, F01030 (2012).
270. Bertello, L., Berti, M., Castellaro, S. & Squarzoni, G. Dynamics of an active earthflow inferred from surface-wave monitoring. *J. Geophys. Res. Earth Surf.* **123**, 1811–1834 (2018).
271. Garcimartin, A., Guarino, A., Bellon, L. & Ciliberto, S. Statistical properties of fracture precursors. *Phys. Rev. Lett.* **79**, 3202–3205 (1997).
272. Sequeiros, O. E. et al. Characteristics of velocity and excess density profiles of saline underflows and turbidity currents flowing over a mobile bed. *J. Hydraul. Eng.* **136**, 412–433 (2010).
273. Majmudar, T. S. & Behringer, R. P. Contact force measurements and stress-induced anisotropy in granular materials. *Nature* **435**, 1079–1082 (2005).

Acknowledgements
The idea for this manuscript originated at the Physics of Dense Suspensions program at the Kavli Institute for Theoretical Physics, supported by the National Science Foundation (PHY-1748958). The authors are grateful to all participants of that workshop, especially the organizers: Bulbul Chakraborty, Emanuela Del Gado and Jeff Morris. D.J.J. was sponsored by the Army Research Office (W911-NF-16-1-0290), the National Science Foundation (NRI INT 1734355) and the US National Institute of Environmental Health Sciences (P42ES02372). K.E.D. is grateful for support from the National Science Foundation (DMR-1206808 and DMR-1608097), the International Fine Particle Research Institute and the James S. McDonnell Foundation. The authors thank their research groups and also Doug Durian and Paulo Arratia for discussions that contributed to ideas presented here, and Andrew Gunn for creating Fig. 2.

Author contributions
The authors contributed equally to all aspects of the article.

Competing interests
The authors declare no competing interests.

Reviewer information
Nature Reviews Physics thanks E. Brodsky, A. Kudrolli and the other, anonymous, reviewer(s) for their contribution to the peer review of this work.